Probing the Protonation and Reduction of Heptavalent Neptunium with Computational Guidance

Grant C. Benthin[a†], Harindu Rajapaksha[a†], Emma L. Markun[a], Sara E. Mason*[a,b], Tori Z. Forbes*[a]

[a] *Department of Chemistry, University of Iowa, Iowa City, IA 52242, USA*
[b] *Center for Functional Nanomaterials, Brookhaven National Laboratory, Upton, NY 11973, USA*

[†]These authors contributed equally to this work and share first authorship

*Corresponding Authors: Tori Z. Forbes Email: tori-forbes@uiowa.edu, Sara E. Mason Email: smason@bnl.gov

Supporting Information

Table of Contents

1. Computational calculations

1.1 DFT optimized coordinates and optimized bond lengths

Table S1: DFT optimized XYZ coordinates of $[NpO_4(OH)_2]^{3-}_{(aq)}$

Np	-5.54480	-0.88550	0.00070
O	-5.53080	1.01120	0.04600
O	-3.65210	-0.90000	-0.10570
O	-7.44140	-0.87330	-0.05610
O	-5.55720	-2.77750	0.11800
O	-5.50380	-0.83880	2.40210
H	-5.47450	0.09180	2.64480
O	-5.57580	-0.94240	-2.40030
H	-6.50500	-0.95730	-2.64950

Table S2: DFT optimized XYZ coordinates of $[NpO_4(OH)(H_2O)]^{2-}_{(aq)}$

Np	-5.58390	-0.91400	-0.12010
O	-5.59090	0.96260	0.01700
O	-3.71020	-0.90790	-0.12420
O	-7.45720	-0.92010	-0.13230
O	-5.57730	-2.78870	0.02820
O	-5.57750	-0.82620	2.55270
H	-5.26900	0.04990	2.81440
O	-5.56810	-0.92150	-2.46450
H	-6.47390	-0.92820	-2.78850
H	-4.96430	-1.45050	2.95900

Table S3: DFT optimized XYZ coordinates of $[NpO_4(H_2O)_2]^{-}_{(aq)}$

Np	-5.61390	-0.86640	0.00870
O	-5.55340	0.98750	-0.01580
O	-3.76290	-0.92750	-0.10480
O	-7.46820	-0.80990	0.01090
O	-5.66770	-2.71620	0.14570
O	-5.53370	-0.75760	2.60640
H	-5.06010	0.00240	2.96590
O	-5.70910	-0.97810	-2.58880
H	-6.48200	-1.43180	-2.94650
H	-5.14760	-1.53390	3.03010
H	-4.94340	-1.39310	-3.00430

Table S4: DFT optimized XYZ coordinates of $[NpO_3(OH)(H_2O)_2]_{(aq)}$

Np	-5.67260	-0.86760	0.01980
O	-5.52820	0.90510	-0.14530
O	-3.56570	-0.88720	-0.13810
O	-7.50370	-0.81160	0.14880
O	-5.59560	-2.64760	0.17530
O	-5.45350	-0.67300	2.52470
H	-5.10530	0.13760	2.91660
O	-5.83230	-1.11310	-2.48670
H	-5.48150	-1.90450	-2.91390
H	-5.07760	-1.40570	3.02840
H	-5.60540	-0.36900	-3.05820
H	-3.20940	-1.78430	-0.08560

Table S5: DFT optimized XYZ coordinates of $trans[NpO_2(OH)_2(H_2O)_2]^{+}_{(aq)}$

Np	-5.37350	-0.88880	-0.04330
O	-5.58000	0.84000	-0.07830
O	-3.31890	-0.68060	0.02720
O	-7.41930	-1.11040	0.05160
O	-5.19120	-2.61440	0.10430
O	-5.34650	-0.71170	2.37770
H	-5.73580	0.03320	2.85460
O	-6.02640	-0.97470	-2.46430
H	-6.79860	-1.50710	-2.69760
H	-5.34620	-1.47190	2.97440
H	-5.35860	-1.13310	-3.14580
H	-2.77630	-1.48360	0.06970
H	-7.97960	-0.31870	0.03020

Table S6: DFT optimized XYZ coordinates of $cis[NpO_2(OH)_2(H_2O)_2]^{+}_{(aq)}$

Np	-5.45620	-0.76140	0.05130
O	-5.66690	1.21900	-0.31940
O	-3.49280	-0.45570	-0.32610
O	-7.21950	-0.68660	0.18180
O	-5.05230	-2.47650	0.21300
O	-5.73170	-1.06590	2.54730
H	-6.17600	-0.38200	3.06570
O	-5.74440	-1.17110	-2.32370
H	-6.48490	-0.84780	-2.85260
H	-4.98870	-1.38180	3.07840
H	-5.32440	-1.89150	-2.81060
H	-2.85910	-1.18640	-0.25280
H	-4.80890	1.65230	-0.47700

Table S7: DFT optimized XYZ coordinates of $[NpO(OH)_3(H_2O)_2]^{2+}_{(aq)}$

Np	-5.34860	-0.99270	0.10740
O	-5.64970	0.96560	-0.05350
O	-3.54820	-0.63880	-0.49910
O	-7.04020	-1.28360	0.35410
O	-5.07170	-2.95530	-0.08400
O	-5.68040	-0.46660	2.49810
H	-4.94440	-0.24790	3.08680
O	-5.83950	-1.04240	-2.21560
H	-6.54210	-1.58670	-2.59970
H	-6.36850	-0.89470	3.02580
H	-5.16230	-0.90660	-2.89440
H	-2.78310	-1.24880	-0.44020
H	-4.93290	1.59530	-0.26380
H	-5.71630	-3.64940	0.15120

Table S8: DFT optimized XYZ coordinates of $[Np(OH)_4(H_2O)_2]^{3+}_{(aq)}$

Np	-5.73310	-1.17770	0.18180
O	-5.99580	0.72990	0.15300
O	-3.83640	-0.90480	-0.00720
O	-7.60400	-1.33900	-0.28570
O	-5.44580	-3.03200	-0.26890
O	-5.20720	-0.40460	2.41150
H	-5.29680	0.50910	2.72390
O	-5.62680	-0.92090	-2.13720
H	-6.35140	-1.18480	-2.72690
H	-4.55160	-0.85580	2.96780
H	-4.80190	-0.89750	-2.64870
H	-3.05020	-1.49330	0.07240
H	-5.35910	1.46810	0.00370
H	-5.98920	-3.83180	-0.07510
H	-8.38860	-0.78760	-0.05910

Table S9: DFT optimized XYZ coordinates of $[NpO_3(OH)_3]^{2-}_{(aq)}$

Np	-5.56930	-0.80760	-0.01860
O	-5.60970	1.01360	0.04970
O	-3.67730	-0.88670	-0.17010
O	-7.77750	-0.74620	0.15020
O	-5.75330	-2.61860	-0.06900
O	-5.43510	-0.90660	2.26020
H	-5.24630	-0.04430	2.64410
O	-5.77950	-0.69730	-2.28960
H	-5.71320	-1.56770	-2.69540
H	-8.05100	0.17660	0.20150

Table S10: DFT optimized XYZ coordinates of $cis[NpO_2(OH)_4]^-_{(aq)}$

Np	-5.45420	-0.81760	-0.01990
O	-5.66200	0.98350	-0.17620
O	-3.67940	-1.19510	-0.14200
O	-7.54920	-0.88650	0.17070
O	-5.59610	-2.91710	0.19610
O	-5.18840	-0.55590	2.13700
H	-5.69600	0.18040	2.49850
O	-5.56870	-0.97220	-2.19970
H	-6.14430	-0.30980	-2.60030
H	-8.01840	-0.04460	0.13050
H	-6.53540	-3.13280	0.30170

Table S11: DFT optimized XYZ coordinates of $trans[NpO_2(OH)_4]^-_{(aq)}$

Np	-5.63020	-0.95350	0.04150
O	-5.63080	0.81150	-0.15270
O	-3.46170	-0.97980	-0.09260
O	-7.79830	-0.90930	0.17460
O	-5.62550	-2.71910	0.23580
O	-5.49070	-0.74660	2.20190
H	-5.54640	0.16140	2.52280
O	-5.76320	-1.22650	-2.11220
H	-5.88280	-0.41060	-2.61280
H	-8.19800	-0.03430	0.11020
H	-3.05230	-1.85060	-0.03210

Table S12: DFT optimized XYZ coordinates of $[NpO(OH)_5]_{(aq)}$

Np	-5.50610	-0.81430	0.06160
O	-5.56640	0.96190	0.05650
O	-3.41070	-0.77160	0.06710
O	-7.58710	-0.82680	-0.04630
O	-5.44550	-2.81900	0.20530
O	-5.51550	-0.73260	2.14780
H	-5.62860	0.10470	2.61740
O	-5.44830	-1.03710	-2.01500
H	-6.19150	-0.73470	-2.55630
H	-8.09130	-0.01510	0.10230
H	-2.94550	-1.60280	-0.10550
H	-5.48430	-3.33300	-0.61800

Table S13: DFT optimized XYZ coordinates of $[Np(OH)_6]^{+}_{(aq)}$

Np	-5.46440	-0.86990	-0.04740
O	-5.47310	1.13800	0.01790
O	-3.44970	-0.87560	-0.14620
O	-7.47390	-0.84960	-0.11720
O	-5.49130	-2.88470	0.06550
O	-5.34750	-0.89660	1.96500
H	-5.49840	-0.09610	2.49800
O	-5.41030	-0.89690	-2.06250
H	-6.20410	-1.07960	-2.59590
H	-8.02540	-0.14770	0.27100
H	-2.88970	-1.16610	0.59450
H	-6.00060	-3.45910	-0.53290
H	-4.81760	1.73850	-0.37620

Table S14: DFT optimized XYZ coordinates of $[NpO_3(OH)_2(H_2O)]^{-}_{(aq)}$

Np	-5.56120	-0.89710	-0.15960
O	-5.81350	0.88090	-0.34720
O	-3.70150	-0.75140	-0.27660
O	-7.69100	-1.06100	0.19630
O	-5.52120	-2.68020	0.10970
O	-5.32070	-0.55750	2.40520
H	-4.79330	0.20080	2.68590
O	-5.83300	-1.22960	-2.35460
H	-5.85320	-0.42670	-2.88500
H	-8.11280	-0.19990	0.08670
H	-4.97720	-1.31400	2.89680

Table S15: DFT optimized XYZ coordinates of $cis[NpO_3(OH)_3(H_2O)]_{(aq)}$

Np	-5.52410	-0.87970	-0.08990
O	-5.57930	0.91280	-0.19290
O	-3.75560	-1.20710	-0.11390
O	-7.56450	-0.83890	0.15000
O	-5.66500	-2.92660	0.09550
O	-5.29500	-0.69200	2.40990
H	-5.68710	0.05780	2.87580
O	-5.66460	-1.01470	-2.23020
H	-6.07940	-0.29260	-2.71640
H	-8.05070	-0.02580	-0.04610
H	-6.59440	-3.19890	0.17410
H	-4.43440	-0.85180	2.81810

Table S16: DFT optimized XYZ coordinates of $trans[NpO_3(OH)_3(H_2O)]_{(aq)}$

Np	-5.65610	-0.95090	-0.05100
O	-5.65720	0.79980	-0.20560
O	-3.54160	-0.98220	-0.04990
O	-7.76190	-0.90420	0.13110
O	-5.64510	-2.68800	0.22790
O	-5.53870	-0.67690	2.43660
H	-5.22210	0.15180	2.81900
O	-5.73520	-1.18970	-2.16880
H	-5.98550	-0.46940	-2.75910
H	-8.21450	-0.07430	-0.07020
H	-3.10180	-1.84240	-0.02500
H	-5.18770	-1.38970	2.98590

Table S17: DFT optimized XYZ coordinates of $[NpO_2(OH)_4(H_2O)]^+_{(aq)}$

Np	-5.61710	-1.01000	-0.04580
O	-5.52510	0.73580	-0.16600
O	-3.60060	-1.26830	-0.09500
O	-7.63820	-0.90440	0.17650
O	-5.80010	-2.95080	0.26050
O	-5.45400	-0.61590	2.35800
H	-5.07620	0.20170	2.71020
O	-5.73530	-1.07620	-2.09740
H	-5.84650	-0.37540	-2.75440
H	-8.15760	-0.12870	-0.09240
H	-2.96870	-0.70300	-0.56860
H	-5.02460	-3.53670	0.17530
H	-5.26200	-1.32200	2.99060

Table S18: DFT optimized XYZ coordinates of $[NpO_2(OH)_5(H_2O)]^{2+}_{(aq)}$

Np	-5.37980	-0.91620	-0.04990
O	-5.25720	1.04340	-0.04570
O	-3.49710	-1.16690	-0.60950
O	-7.31870	-0.74150	0.20980
O	-5.74610	-2.85370	-0.01270
O	-5.61820	-0.92060	2.35470
H	-6.33790	-0.45450	2.80540
O	-5.71620	-0.85310	-2.02570
H	-6.50570	-0.89350	-2.59320
H	-7.78770	0.11820	0.23780
H	-2.78780	-1.31560	0.05240
H	-5.08220	-3.55370	-0.17870
H	-4.72800	1.64480	-0.60680
H	-4.82480	-0.85680	2.90990

Table S19: DFT optimized XYZ coordinates of $[NpO_4(OH)_2]^{4-}_{(aq)}$

Np	-5.64285	-0.75438	-0.00445
O	-5.71984	1.21617	-0.15277
O	-3.67926	-0.66146	0.10958
O	-7.60528	-0.84664	-0.11876
O	-5.56703	-2.72497	0.14315
O	-5.77880	-0.56630	2.47521
H	-4.85273	-0.58263	2.73577
O	-5.51778	-0.95125	-2.48564
H	-6.42189	-1.20021	-2.70208

Table S20: DFT optimized XYZ coordinates of $[NpO_4(OH)(H_2O)]^{3-}_{(aq)}$

Np	-6.09583	-1.70040	-0.06916
O	-6.69611	-0.22262	1.10422
O	-4.41874	-1.76940	0.95175
O	-7.80930	-1.69789	-0.96036
O	-5.60279	-3.32128	-1.01679
O	-4.54852	0.40446	2.55130
H	-5.44946	0.37403	2.12153
O	-5.13328	-0.24579	-1.66879
H	-5.79059	-0.06271	-2.34691
H	-4.22758	-0.40301	2.07487

Table S21: DFT optimized XYZ coordinates of $[NpO_4(H_2O)_2]^{2-}_{(aq)}$

Np	-4.77968	-1.71471	0.00211
O	-4.67059	0.22993	0.26359
O	-2.88636	-1.83808	0.20160
O	-6.72586	-1.56462	-0.24329
O	-4.90353	-3.60447	-0.22406
O	-5.50378	-0.83879	2.40203
H	-5.22241	-0.11921	1.74987
O	-5.57582	-0.94237	-2.40019
H	-6.32347	-1.11761	-1.73952
H	-4.83779	-0.84439	3.09945
H	-5.64796	-1.62299	-3.07931

Table S22: DFT optimized XYZ coordinates of $[NpO_3(OH)(H_2O)_2]^-_{(aq)}$

Np	-6.00580	-0.85739	0.06063
O	-5.96241	0.96857	-0.02817
O	-3.79319	-0.79493	-0.55130
O	-7.88997	-0.90398	0.36287
O	-5.82596	-2.67736	0.15908
O	-5.32235	-0.70572	2.52776
H	-4.91392	0.11793	2.82112
O	-5.50485	-0.87108	-2.60085
H	-5.59706	-1.73587	-3.01773
H	-4.78533	-1.41975	2.89234
H	-4.61308	-0.86281	-2.17288
H	-3.41686	-1.67853	-0.46694

Table S23: DFT optimized XYZ coordinates of $trans[NpO_2(OH)_2(H_2O)_2]_{(aq)}$

Np	-5.37283	-0.81957	0.06034
O	-5.60890	0.93906	0.01483
O	-3.22699	-0.54086	0.15664
O	-7.52020	-1.11154	-0.01772
O	-5.14868	-2.57728	0.15055
O	-5.55488	-0.79779	2.55085
H	-5.45441	0.00410	3.07816
O	-5.96295	-0.97682	-2.45097
H	-6.86151	-1.33389	-2.45182
H	-5.23232	-1.53277	3.08667
H	-5.44239	-1.53400	-3.04347
H	-2.71301	-1.35531	0.21371
H	-8.04506	-0.30239	-0.04185

Table S24: DFT optimized XYZ coordinates of $cis[NpO_2(OH)_2(H_2O)_2]_{(aq)}$

Np	-5.63974	-0.90506	0.00179
O	-5.85367	1.18750	-0.06899
O	-3.56933	-0.59203	-0.12607
O	-7.46371	-0.96422	0.01624
O	-5.32105	-2.69877	0.12073
O	-5.51268	-0.78477	2.51913
H	-5.48439	0.07044	2.96618
O	-5.69469	-0.98621	-2.51629
H	-6.53869	-1.14290	-2.95796
H	-4.90160	-1.36424	2.99087
H	-5.03395	-1.50405	-2.99318
H	-3.00407	-1.37269	-0.06882
H	-4.98812	1.62159	-0.10850

Table S25: DFT optimized XYZ coordinates of $[NpO(OH)_3(H_2O)_2]^+_{(aq)}$

Np	-5.49938	-1.07438	-0.11021
O	-5.75937	0.99191	-0.01904
O	-3.54157	-0.75917	-0.10554
O	-7.24870	-1.26772	-0.09692
O	-5.18404	-3.01835	0.55209
O	-5.55591	-0.73102	2.33372
H	-5.50848	0.17191	2.67434
O	-5.81456	-0.79479	-2.56045
H	-6.61880	-1.10845	-2.99385
H	-5.02701	-1.28930	2.91823
H	-5.09158	-0.89595	-3.19372
H	-2.91201	-1.47815	0.07673
H	-4.95948	1.53960	-0.02448
H	-5.90712	-3.63861	0.72207

Table S26: DFT optimized XYZ coordinates of $[Np(OH)_4(H_2O)_2]^{2+}_{(aq)}$

Np	-5.42519	-1.03048	0.09892
O	-5.72919	0.91759	0.03595
O	-3.54105	-0.72610	-0.44859
O	-7.38026	-1.31023	0.11920
O	-5.16874	-2.97964	-0.13989
O	-5.71987	-0.55610	2.50425
H	-5.73792	0.33798	2.87137
O	-5.75537	-1.00986	-2.25855
H	-6.51683	-1.43502	-2.67838
H	-5.48017	-1.16796	3.21343
H	-5.00815	-1.06215	-2.87181
H	-2.82791	-1.39139	-0.42601
H	-5.04244	1.59632	-0.10580
H	-5.83863	-3.65848	0.06722
H	-8.06608	-0.64733	0.32378

Table S27: DFT optimized XYZ coordinates of $[NpO_3(OH)_3]^{3-}_{(aq)}$

Np	-5.42404	-0.90455	0.01906
O	-5.53441	0.97164	0.00687
O	-3.45975	-0.90501	-0.08372
O	-7.73638	-0.89837	-0.03846
O	-5.52570	-2.77498	0.12142
O	-5.47088	-0.84349	2.38319
H	-5.41698	0.07981	2.64882
O	-5.56309	-0.97813	-2.37410
H	-6.50035	-0.86464	-2.56556
H	-7.98056	0.03292	-0.05447

Table S28: DFT optimized XYZ coordinates of $cis[NpO_2(OH)_4]^{2-}_{(aq)}$

Np	-5.45248	-0.78850	-0.00432
O	-5.51054	1.08590	-0.05601
O	-3.58953	-0.97744	-0.09764
O	-7.63624	-0.83056	-0.01077
O	-5.57550	-2.97063	0.16829
O	-5.44184	-0.68711	2.26406
H	-5.42414	0.21540	2.59663
O	-5.54060	-0.94578	-2.27184
H	-6.37548	-0.60162	-2.60736
H	-8.03593	0.04109	0.07932
H	-6.50977	-3.20847	0.23600

Table S29: DFT optimized XYZ coordinates of $trans[NpO_2(OH)_4]^{2-}_{(aq)}$

Np	-5.64364	-0.80523	0.02585
O	-5.52899	1.00299	0.07556
O	-3.38573	-0.92869	-0.07318
O	-7.90151	-0.68177	0.12488
O	-5.75828	-2.61344	-0.02387
O	-5.54558	-0.89029	2.28815
H	-5.46954	-0.01053	2.67170
O	-5.74168	-0.72015	-2.23645
H	-5.81769	-1.59993	-2.62000
H	-8.20371	0.23161	0.16003
H	-3.08359	-1.84209	-0.10830

Table S30: DFT optimized XYZ coordinates of $[NpO(OH)_5]^{-}_{(aq)}$

Np	-5.54511	-0.83819	0.05437
O	-5.61892	0.96398	-0.08543
O	-3.37281	-0.74536	-0.02951
O	-7.70831	-0.91989	0.11889
O	-5.44857	-2.89956	0.24935
O	-5.45948	-0.72016	2.20918
H	-5.50516	0.14443	2.63171
O	-5.60821	-1.12617	-2.08450
H	-5.86121	-0.40015	-2.66477
H	-8.17612	-0.07811	0.09012
H	-2.94388	-1.60912	0.00240
H	-5.57294	-3.39209	-0.57490

Table S31: DFT optimized XYZ coordinates of $[Np(OH)_6]_{(aq)}$

Np	-5.52193	-0.89686	-0.06107
O	-5.38026	1.15971	0.09578
O	-3.47333	-1.15519	-0.23286
O	-7.58616	-0.72044	-0.03591
O	-5.82367	-2.95035	-0.13830
O	-5.32920	-1.00612	2.00136
H	-5.48321	-0.21817	2.54219
O	-5.53588	-0.75879	-2.12994
H	-6.35968	-0.87589	-2.62357
H	-7.99151	0.13791	0.15283
H	-2.94261	-1.23825	0.57246
H	-5.07673	-3.54967	0.00137
H	-5.04196	1.72666	-0.61075

Table S32: DFT optimized XYZ coordinates of $[NpO_3(OH)_2(H_2O)]^{2-}_{(aq)}$

Np	-6.06362	-1.60759	-0.00860
O	-6.51901	-0.03718	0.85770
O	-4.33783	-1.70204	0.94897
O	-8.19659	-1.72008	-0.76237
O	-5.77247	-3.19127	-0.89920
O	-4.01972	0.56172	2.29620
H	-4.90552	0.86360	2.05062
O	-5.33447	-0.44771	-1.82124
H	-5.33798	0.50055	-1.65845
H	-8.66577	-0.93001	-0.47264
H	-4.02576	-0.32575	1.82660

Table S33: DFT optimized XYZ coordinates of $cis[NpO_3(OH)_3(H_2O)]^{-}_{(aq)}$

Np	-5.53676	-0.90751	-0.10815
O	-5.51674	0.93909	-0.18717
O	-3.69922	-1.15144	-0.11002
O	-7.65685	-0.83557	0.23355
O	-5.70522	-3.03927	0.07757
O	-5.26538	-0.73393	2.47923
H	-5.79614	-0.06085	2.92321
O	-5.78017	-1.07080	-2.30505
H	-5.86532	-0.25055	-2.80004
H	-8.08045	0.01542	0.07342
H	-6.63968	-3.28850	0.10905
H	-4.35232	-0.57375	2.74859

Table S34: DFT optimized XYZ coordinates of $trans[NpO_3(OH)_3(H_2O)]^-_{(aq)}$

Np	-5.68284	-0.79017	-0.10822
O	-5.58125	1.00013	-0.06443
O	-3.47807	-0.90452	0.02587
O	-7.87807	-0.67888	0.13607
O	-5.78065	-2.58017	-0.06095
O	-5.59181	-0.78514	2.48781
H	-5.23795	0.01864	2.88865
O	-5.74839	-0.76508	-2.31936
H	-5.79554	-1.62913	-2.74108
H	-8.22537	0.21981	0.13498
H	-3.13379	-1.80389	-0.00470
H	-5.11372	-1.51765	2.89611

Table S35: DFT optimized XYZ coordinates of $[NpO_2(OH)_4(H_2O)]_{(aq)}$

Np	-5.51424	-0.87441	-0.07983
O	-5.65262	0.90489	-0.06859
O	-3.40513	-0.68445	-0.01714
O	-7.59976	-1.09268	0.08019
O	-5.30084	-2.89129	0.04101
O	-5.47784	-0.64920	2.43430
H	-5.15404	0.18312	2.80196
O	-5.57801	-0.96122	-2.19945
H	-5.74405	-0.19826	-2.76334
H	-8.21198	-0.36696	-0.09307
H	-2.90537	-1.51135	-0.06516
H	-6.04972	-3.45714	-0.20282
H	-5.11247	-1.35496	2.98361

Table S36: DFT optimized XYZ coordinates of $[NpO_2(OH)_5(H_2O)]^+_{(aq)}$

Np	-5.57400	-0.92839	-0.03385
O	-5.54381	1.08577	-0.11024
O	-3.56729	-1.11119	-0.00336
O	-7.59025	-0.83742	0.09875
O	-5.77579	-2.91895	0.28784
O	-5.55212	-0.72717	2.39833
H	-5.19235	0.05809	2.83415
O	-5.52908	-1.10079	-2.06619
H	-5.99215	-0.69092	-2.80852
H	-8.05746	0.00125	-0.05275
H	-2.98660	-1.15873	-0.77976
H	-5.04893	-3.54832	0.15073
H	-4.81780	1.64538	-0.43042
H	-5.35976	-1.48852	2.96323

Table S37: DFT optimized XYZ coordinates of $H_3O^+_{(aq)}$

O	-0.17411	-1.45771	0.22714
H	0.74696	-1.58807	-0.07859
H	-0.52041	-0.59421	-0.07786
H	-0.74876	-2.18866	-0.08011

Table S38: DFT optimized XYZ coordinates of $H_2O_{(aq)}$

O	-0.17854	-1.52568	0.00000
H	0.78474	-1.48419	0.00000
H	-0.46098	-0.60380	0.00000

Table S39: DFT optimized XYZ coordinates of $OH^-_{(aq)}$

O	-0.69144	-0.16869	0.00000
H	-1.01342	0.74054	0.00000

Table S40: DFT optimized XYZ coordinates of $O^{2-}_{2(aq)}$

O	-0.26678	-1.08410	0.00000
O	1.33218	-1.19438	0.00000

Table S41: DFT optimized XYZ coordinates of $O^{-*}_{2(aq)}$

O	-0.13941	-1.09289	0.00000
O	1.20481	-1.18559	0.00000

Table S42: DFT optimized XYZ coordinates of $HO^-_{2(aq)}$

O	-0.35439	-1.00051	-0.07295
O	1.13213	-1.28232	0.09570
H	-0.69145	-1.64622	0.55633

Table S43: DFT optimized XYZ coordinates of $NO^-_{3(aq)}$

O	1.23976	0.18942	0.00003
O	-0.45584	-1.16847	0.00003
O	-0.78390	0.97906	0.00003
N	-0.00003	-0.00001	0.00003

Table S44: DFT optimized XYZ coordinates of $NO^*_{3(aq)}$

O	1.21520	0.18942	0.00001
O	-0.44333	-1.14733	0.00005
O	-0.77152	0.95794	0.00002
N	-0.00035	-0.00003	0.00003

Table S45: DFT optimized XYZ coordinates of $CO^{2-}_{3(aq)}$

C	-0.45247	-0.48135	-2.21460
O	0.19389	0.64234	-2.21460
O	0.19370	-1.60513	-2.21460

O	-1.74951	-0.48125	-2.21460

Table S46: DFT optimized XYZ coordinates of $CO_{3(aq)}^{-*}$

C	-0.45359	-0.48134	-2.21460
O	0.18472	0.61655	-2.21460
O	0.17803	-1.58310	-2.21460
O	-1.72355	-0.47751	-2.21460

Table S47: DFT optimized XYZ coordinates of $[Co(NH_3)_6]_{(aq)}^{3+}$

Co	-1.73560	0.93209	-0.00567
N	-1.75904	0.91786	2.02882
H	-2.43523	0.26431	2.43142
H	-0.86739	0.66246	2.45993
N	-1.71230	0.94640	-2.04017
H	-2.60362	1.20322	-2.47114
H	-1.03518	1.59896	-2.44281
N	-1.77303	-1.10208	-0.03237
H	-2.44202	-1.49619	-0.69839
H	-0.87913	-1.53076	-0.28460
N	-3.76966	0.98192	-0.01662
H	-4.18393	1.23594	0.88355
H	-4.16477	1.65461	-0.67829
N	-1.69797	2.96624	0.02092
H	-1.03019	3.36029	0.68818
H	-1.45068	3.39601	-0.87367
N	0.29844	0.88222	0.00538
H	0.74162	1.77137	0.24855
H	0.69344	0.20928	0.66687
H	0.71280	0.62849	-0.89482
H	-4.21285	0.09268	-0.25942
H	-2.01850	-1.53201	0.86264
H	-1.99573	1.82046	2.44803
H	-2.59227	3.39514	0.27136
H	-1.47707	0.04347	-2.45950

Table S48: DFT optimized XYZ coordinates of $[Co(NH_3)_6Cl]^{2+}_{(aq)}$

Co	-1.75576	0.98169	-0.00595
N	-1.77837	0.89899	2.00823
H	-2.09406	-0.04414	2.24442
H	-0.86702	0.99879	2.45391
N	-1.75744	0.90614	-2.02060
H	-2.61195	1.23061	-2.47137
H	-0.99858	1.38960	-2.49950
N	-3.77313	0.98979	-0.01186
H	-4.21231	1.27032	0.86418
H	-4.23035	1.54279	-0.73593
N	-1.64490	3.03698	-0.00596
H	-1.24224	3.42111	0.84855
H	-1.07213	3.40968	-0.76278
N	0.25137	0.80641	0.01458
H	0.76685	1.44793	0.61640
H	0.44591	-0.14319	0.33862
H	0.69554	0.87100	-0.90043
H	-4.04681	0.01628	-0.16368
H	-2.39355	1.55444	2.48929
H	-2.55034	3.49544	-0.10431
H	-1.67386	-0.08582	-2.25451
Cl	-1.85370	-1.24505	-0.00726

Table S49: DFT optimized XYZ coordinates of $cis[Co(NH_3)_6Cl_2]^{+}_{(aq)}$

Co	-1.75918	0.98428	-0.02596
N	-1.76373	0.85647	-2.05880
H	-2.57197	1.25713	-2.52789
H	-0.94159	1.22552	-2.52967
N	-3.75374	0.93620	0.06887
H	-3.98907	1.15924	1.03545
H	-4.31867	1.51785	-0.54439
N	-1.71956	3.02096	-0.04511
H	-1.71209	3.25153	0.94990
H	-0.89709	3.44622	-0.46527
N	0.23221	0.85909	0.06505
H	0.47781	1.07313	1.03110
H	0.45308	-0.12519	-0.08271
H	0.81813	1.41816	-0.54951
H	-4.01292	-0.03869	-0.07882
H	-2.52749	3.47800	-0.46010
H	-1.78344	-0.15232	-2.21760
Cl	-1.80259	-1.26157	-0.02994
Cl	-1.75371	1.15108	2.21420

Table S50: DFT optimized XYZ coordinates of $trans[Co(NH_3)_6Cl_2]^+_{(aq)}$

Co	-1.74633	0.91906	-0.00851
N	-1.73801	0.94223	1.98484
H	-2.25226	0.14144	2.34668
H	-0.80627	0.88762	2.38766
N	-1.75465	0.89589	-2.00186
H	-2.68640	0.95047	-2.40469
H	-1.24042	1.69669	-2.36371
N	-3.73533	1.05204	-0.00202
H	-4.13686	1.08920	0.93114
H	-4.03087	1.90468	-0.47350
N	0.24267	0.78608	-0.01501
H	0.65000	1.60188	0.43795
H	0.53821	-0.06658	0.45643
H	0.64420	0.74898	-0.94817
H	-4.14266	0.23623	-0.45493
H	-2.14563	1.81012	2.32719
H	-1.34701	0.02800	-2.34421
Cl	-1.89625	-1.32632	0.01804
Cl	-1.59641	3.16444	-0.03507

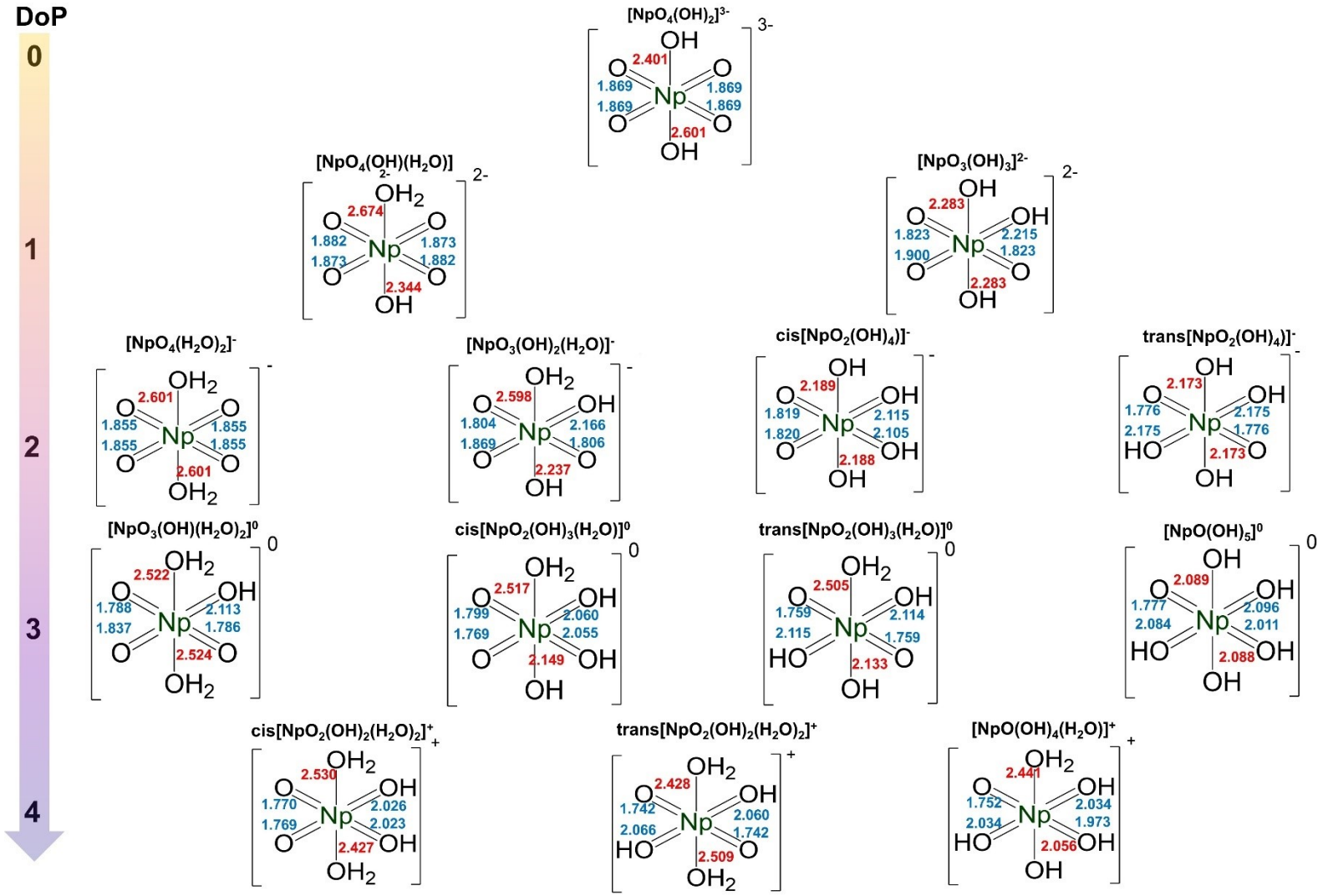

Figure S1: DFT optimized bond lengths. Here DoP stands for Degree of Protonation

1.2 Np(VII) Protonation reactions and their energetics.

Table S51: Protonation reactions of Np(VII) complexes

Δ DoP	Reaction	ΔG (kJ/mol)
0→1	$[NpO_4(OH)_2]^{3-}_{(aq)} + H_3O^+_{(aq)} \rightarrow [NpO_4(OH)(H_2O)]^{2-}_{(aq)} + H_2O_{(aq)}$	-326.23
0→1	$[NpO_4(OH)_2]^{3-}_{(aq)} + H_3O^+_{(aq)} \rightarrow [NpO_3(OH)_3]^{2-}_{(aq)} + H_2O_{(aq)}$	-291.20
1→2	$[NpO_4(OH)(H_2O)]^{2-}_{(aq)} + H_3O^+_{(aq)} \rightarrow [NpO_4(H_2O)_2]^-_{(aq)} + H_2O_{(aq)}$	-260.60
1→2	$[NpO_4(OH)(H_2O)]^{2-}_{(aq)} + H_3O^+_{(aq)} \rightarrow [NpO_3(OH)_2(H_2O)]^-_{(aq)} + H_2O_{(aq)}$	-267.18
1→2	$[NpO_3(OH)_3]^{2-}_{(aq)} + H_3O^+_{(aq)} \rightarrow cis[NpO_2(OH)_4]^-_{(aq)} + H_2O_{(aq)}$	-182.54
1→2	$[NpO_3(OH)_3]^{2-}_{(aq)} + H_3O^+_{(aq)} \rightarrow trans[NpO_2(OH)_4]^-_{(aq)} + H_2O_{(aq)}$	-252.16
2→3	$[NpO_4(H_2O)_2]^-_{(aq)} + H_3O^+_{(aq)} \rightarrow [NpO_3(OH)(H_2O)_2]_{(aq)} + H_2O_{(aq)}$	-211.69
2→3	$[NpO_3(OH)_2(H_2O)]^-_{(aq)} + H_3O^+_{(aq)} \rightarrow cis[NpO_3(OH)_3(H_2O)]_{(aq)} + H_2O_{(aq)}$	-120.87
2→3	$[NpO_3(OH)_2(H_2O)]^-_{(aq)} + H_3O^+_{(aq)} \rightarrow trans[NpO_3(OH)_3(H_2O)]_{(aq)} ++ H_2O_{(aq)}$	-178.56
2→3	$cis[NpO_2(OH)_4]^-_{(aq)} + H_3O^+_{(aq)} \rightarrow [NpO(OH)_5]_{(aq)} ++ H_2O_{(aq)}$	-127.16
2→3	$trans[NpO_2(OH)_4]^-_{(aq)} + H_3O^+_{(aq)} \rightarrow [NpO(OH)_5]_{(aq)} ++ H_2O_{(aq)}$	-59.15
3→4	$[NpO_3(OH)(H_2O)_2]_{(aq)} + H_3O^+_{(aq)} \rightarrow cis[NpO_2(OH)_2(H_2O)_2]^+_{(aq)} + H_2O_{(aq)}$	-47.43
3→4	$[NpO_3(OH)(H_2O)_2]_{(aq)} + H_3O^+_{(aq)} \rightarrow trans[NpO_2(OH)_2(H_2O)_2]^+_{(aq)} + H_2O_{(aq)}$	-89.63
3→4	$cis[NpO_2(OH)_3(H_2O)]_{(aq)} + H_3O^+_{(aq)} \rightarrow [NpO(OH)_4(H_2O)]^+_{(aq)} + H_2O_{(aq)}$	-45.87
3→4	$trans[NpO_2(OH)_3(H_2O)]_{(aq)} + H_3O^+_{(aq)} \rightarrow [NpO(OH)_4(H_2O)]^+_{(aq)} + H_2O_{(aq)}$	10.97
3→4	$[NpO(OH)_5]_{(aq)} + H_3O^+_{(aq)} \rightarrow [Np(OH)_6]^+_{(aq)} ++ H_2O_{(aq)}$	2.67
4→5	$cis[NpO_2(OH)_2(H_2O)_2]^+_{(aq)} + H_3O^+_{(aq)} \rightarrow [NpO(OH)_3(H_2O)_2]^{2+}_{(aq)} + H_2O_{(aq)}$	52.28
4→5	$trans[NpO_2(OH)_2(H_2O)_2]^+_{(aq)} + H_3O^+_{(aq)} \rightarrow [NpO(OH)_3(H_2O)_2]^{2+}_{(aq)} + H_2O_{(aq)}$	109.82
4→5	$[NpO_2(OH)_4(H_2O)]^+_{(aq)} + H_3O^+_{(aq)} \rightarrow [NpO(OH)_5(H_2O)]^{2+}_{(aq)} + H_2O_{(aq)}$	109.83
4→5	$[Np(OH)_6]^+_{(aq)} + H_3O^+_{(aq)} \rightarrow [NpO(OH)_5(H_2O)]^{2+}_{(aq)} + H_2O_{(aq)}$	16.60
5→6	$[NpO(OH)_3(H_2O)_2]^{2+}_{(aq)} + H_3O^+_{(aq)} \rightarrow [Np(OH)_4(H_2O)_2]^{3+}_{(aq)} + H_2O_{(aq)}$	337.20
5→6	$[NpO(OH)_5(H_2O)]^{2+}_{(aq)} + H_3O^+_{(aq)} \rightarrow [Np(OH)_4(H_2O)_2]^{3+}_{(aq)} + H_2O_{(aq)}$	851.57

Table S52: Protonation reactions of Np(VI) complexes

Δ DoP	Reaction	ΔG (kJ/mol)
0→1	$[NpO_4(OH)_2]^{4-}_{(aq)} + H_3O^+_{(aq)} \rightarrow [NpO_4(OH)(H_2O)]^{3-}_{(aq)} + H_2O_{(aq)}$	-427.37
0→1	$[NpO_4(OH)_2]^{4-}_{(aq)} + H_3O^+_{(aq)} \rightarrow [NpO_3(OH)_3]^{3-}_{(aq)} + H_2O_{(aq)}$	-366.78
1→2	$[NpO_4(OH)(H_2O)]^{3-}_{(aq)} + H_3O^+_{(aq)} \rightarrow [NpO_4(H_2O)_2]^{2-}_{(aq)} + H_2O_{(aq)}$	-310.95
1→2	$[NpO_4(OH)(H_2O)]^{3-}_{(aq)} + H_3O^+_{(aq)} \rightarrow [NpO_3(OH)_2(H_2O)]^{2-}_{(aq)} + H_2O_{(aq)}$	-375.76
1→2	$[NpO_3(OH)_3]^{3-}_{(aq)} + H_3O^+_{(aq)} \rightarrow cis[NpO_2(OH)_4]^{2-}_{(aq)} + H_2O_{(aq)}$	-306.38
1→2	$[NpO_3(OH)_3]^{3-}_{(aq)} + H_3O^+_{(aq)} \rightarrow trans[NpO_2(OH)_4]^{2-}_{(aq)} + H_2O_{(aq)}$	-383.24
2→3	$[NpO_4(H_2O)_2]^{2-}_{(aq)} + H_3O^+_{(aq)} \rightarrow [NpO_3(OH)(H_2O)_2]^-_{(aq)} + H_2O_{(aq)}$	-286.71
2→3	$[NpO_3(OH)_2(H_2O)]^{2-}_{(aq)} + H_3O^+_{(aq)} \rightarrow cis[NpO_3(OH)_3(H_2O)]^-_{(aq)} + H_2O_{(aq)}$	-228.59
2→3	$[NpO_3(OH)_2(H_2O)]^{2-}_{(aq)} + H_3O^+_{(aq)} \rightarrow trans[NpO_3(OH)_3(H_2O)]^-_{(aq)} ++ H_2O_{(aq)}$	-300.16
2→3	$cis[NpO_2(OH)_4]^{2-}_{(aq)} + H_3O^+_{(aq)} \rightarrow [NpO(OH)_5]^-_{(aq)} ++ H_2O_{(aq)}$	-121.35
2→3	$trans[NpO_2(OH)_4]^{2-}_{(aq)} + H_3O^+_{(aq)} \rightarrow [NpO(OH)_5]^-_{(aq)} ++ H_2O_{(aq)}$	-44.48
3→4	$[NpO_3(OH)(H_2O)_2]^-_{(aq)} + H_3O^+_{(aq)} \rightarrow cis[NpO_2(OH)_2(H_2O)_2]_{(aq)} + H_2O_{(aq)}$	-207.00
3→4	$[NpO_3(OH)(H_2O)_2]^-_{(aq)} + H_3O^+_{(aq)} \rightarrow trans[NpO_2(OH)_2(H_2O)_2]_{(aq)} + H_2O_{(aq)}$	-268.26
3→4	$cis[NpO_2(OH)_3(H_2O)]^-_{(aq)} + H_3O^+_{(aq)} \rightarrow [NpO(OH)_4(H_2O)]_{(aq)} + H_2O_{(aq)}$	-188.61
3→4	$trans[NpO_2(OH)_3(H_2O)]^-_{(aq)} + H_3O^+_{(aq)} \rightarrow [NpO(OH)_4(H_2O)]_{(aq)} + H_2O_{(aq)}$	-117.04
3→4	$[NpO(OH)_5]^-_{(aq)} + H_3O^+_{(aq)} \rightarrow [Np(OH)_6]_{(aq)} ++ H_2O_{(aq)}$	-265.18
4→5	$cis[NpO_2(OH)_2(H_2O)_2]_{(aq)} + H_3O^+_{(aq)} \rightarrow [NpO(OH)_3(H_2O)_2]^+_{(aq)} + H_2O_{(aq)}$	-94.05
4→5	$trans[NpO_2(OH)_2(H_2O)_2]_{(aq)} + H_3O^+_{(aq)} \rightarrow [NpO(OH)_3(H_2O)_2]^+_{(aq)} + H_2O_{(aq)}$	-52.93
4→5	$[NpO_2(OH)_4(H_2O)]_{(aq)} + H_3O^+_{(aq)} \rightarrow [NpO(OH)_5(H_2O)]^+_{(aq)} + H_2O_{(aq)}$	-52.93
4→5	$[Np(OH)_6]_{(aq)} + H_3O^+_{(aq)} \rightarrow [NpO(OH)_5(H_2O)]^+_{(aq)} + H_2O_{(aq)}$	-92.39
5→6	$[NpO(OH)_3(H_2O)_2]^+_{(aq)} + H_3O^+_{(aq)} \rightarrow [Np(OH)_4(H_2O)_2]^{2+}_{(aq)} + H_2O_{(aq)}$	12.74
5→6	$[NpO(OH)_5(H_2O)]^+_{(aq)} + H_3O^+_{(aq)} \rightarrow [Np(OH)_4(H_2O)_2]^{2+}_{(aq)} + H_2O_{(aq)}$	541.57

1.3 Influence of protonation on reduction of Np(VII)

Table S53: Free energy changes associated with the reduction of Np(VII) to corresponding Np(VI) compounds with different reducing agents.

Np(VII) reduction half reaction	Reaction ΔG (kJ/mol) Reducing agent					
	$O_{2(aq)}^{2-}$	$HO_{2(aq)}^{-}$	$O_{2(aq)}^{-*}$	$CO_{3(aq)}^{2-}$	$Cl_{(aq)}^{-}$	$NO_{3(aq)}^{-}$
I	-311.44	-124.84	-218.86	384.33	381.76	377.75
II	-384.72	-198.12	-292.13	311.05	308.49	304.47
III	-412.58	-225.98	-320.00	283.19	280.62	276.61
IV	-435.06	-248.47	-342.48	260.70	258.14	254.12
V	-493.29	-306.69	-400.71	202.48	199.91	195.90
VI	-536.42	-349.82	-451.08	159.35	156.78	152.77
VII	-543.66	-357.06	-451.08	152.11	149.54	145.53
VIII	-510.14	-323.54	-417.55	185.63	183.07	179.05
IX	-600.35	-413.75	-507.76	95.42	92.86	88.84
X	-615.08	-428.48	-522.50	80.69	78.12	74.11
XI	-529.00	-342.40	-436.42	166.77	164.20	160.19
XII	-743.08	-556.49	-650.50	-47.32	-49.88	-53.90
XIII	-669.71	-483.11	-577.13	26.06	23.49	19.48
XIV	-688.76	-502.16	-596.18	7.00	4.44	0.43

Table S54: Spin densities and oxidation states of Np centers in Np(VI) and Np(VII) complexes.

Compound	Np Oxidation state	Np Spin Density
$[NpO_4(OH)_2]_{(aq)}^{3-}$	VII	0.000
$[NpO_4(OH)(H_2O)]_{(aq)}^{2-}$	VII	0.000
$[NpO_3(OH)_3]_{(aq)}^{2-}$	VII	0.000
$[NpO_4(H_2O)_2]_{(aq)}^{-}$	VII	0.000
$[NpO_3(OH)_2(H_2O)]_{(aq)}^{-}$	VII	0.000
$cis[NpO_2(OH)_4]_{(aq)}^{-}$	VII	0.000
$trans[NpO_2(OH)_4]_{(aq)}^{-}$	VII	0.000
$[NpO_3(OH)(H_2O)_2]_{(aq)}$	VII	0.000
$cis[NpO_2(OH)_3(H_2O)]_{(aq)}$	VII	0.000
$trans[NpO_2(OH)_3(H_2O)]_{(aq)}$	VII	0.000
$[NpO(OH)_5]_{(aq)} + H_3O_{(aq)}^{+}$	VII	0.000
$cis[NpO_2(OH)_2(H_2O)_2]_{(aq)}^{+}$	VII	0.000
$trans[NpO_2(OH)_2(H_2O)_2]_{(aq)}^{+}$	VII	0.000
$[NpO_2(OH)_4(H_2O)]_{(aq)}^{+}$	VII	0.000
$[Np(OH)_6]_{(aq)}^{+}$	VII	0.000
$[NpO(OH)_3(H_2O)_2]_{(aq)}^{2+}$	VII	0.000
$[NpO(OH)_5(H_2O)]_{(aq)}^{2+}$	VII	0.000

$[Np(OH)_4(H_2O)_2]^{3+}_{(aq)}$	VII	0.000
$[NpO_4(OH)_2]^{4-}_{(aq)}$	VI	1.145
$[NpO_4(OH)(H_2O)]^{3-}_{(aq)}$	VI	1.189
$[NpO_3(OH)_3]^{3-}_{(aq)}$	VI	1.132
$[NpO_4(H_2O)_2]^{2-}_{(aq)}$	VI	1.215
$[NpO_3(OH)_2(H_2O)]^{2-}_{(aq)}$	VI	1.167
$cis[NpO_2(OH)_4]^{2-}_{(aq)}$	VI	1.121
$trans[NpO_2(OH)_4]^{2-}_{(aq)}$	VI	1.198
$[NpO_3(OH)(H_2O)_2]^{-}_{(aq)}$	VI	1.154
$cis[NpO_2(OH)_3(H_2O)\,]^{-}_{(aq)}$	VI	1.178
$trans[NpO_2(OH)_3(H_2O)]^{-}_{(aq)}$	VI	1.139
$[NpO(OH)_5]^{-}_{(aq)}$	VI	1.178
$cis[NpO_2(OH)_2(H_2O)_2]_{(aq)}$	VI	1.139
$trans[NpO_2(OH)_2(H_2O)_2]_{(aq)}$	VI	1.125
$[NpO_2(OH)_4(H_2O)]_{(aq)}$	VI	1.192
$[Np(OH)_6]_{(aq)}$	VI	1.147
$[NpO(OH)_3(H_2O)_2]^{+}_{(aq)}$	VI	1.203
$[NpO(OH)_5(H_2O)]^{+}_{(aq)}$	VI	1.134
$[Np(OH)_4(H_2O)_2]^{+}_{(aq)}$	VI	1.148

1.4 Prediction of Raman spectra

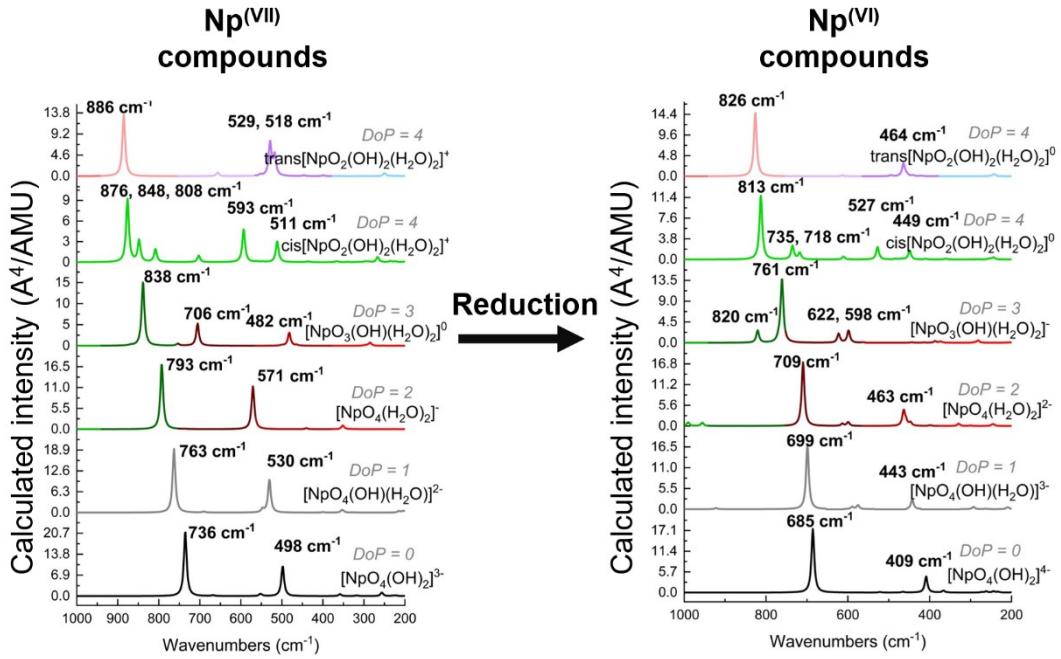

Figure S2: Predicted Raman spectra of Np(VII) and corresponding Np(VI) compounds in protonation path 1 and 2. Here DoP stands for Degree of Protonation. The color of each line

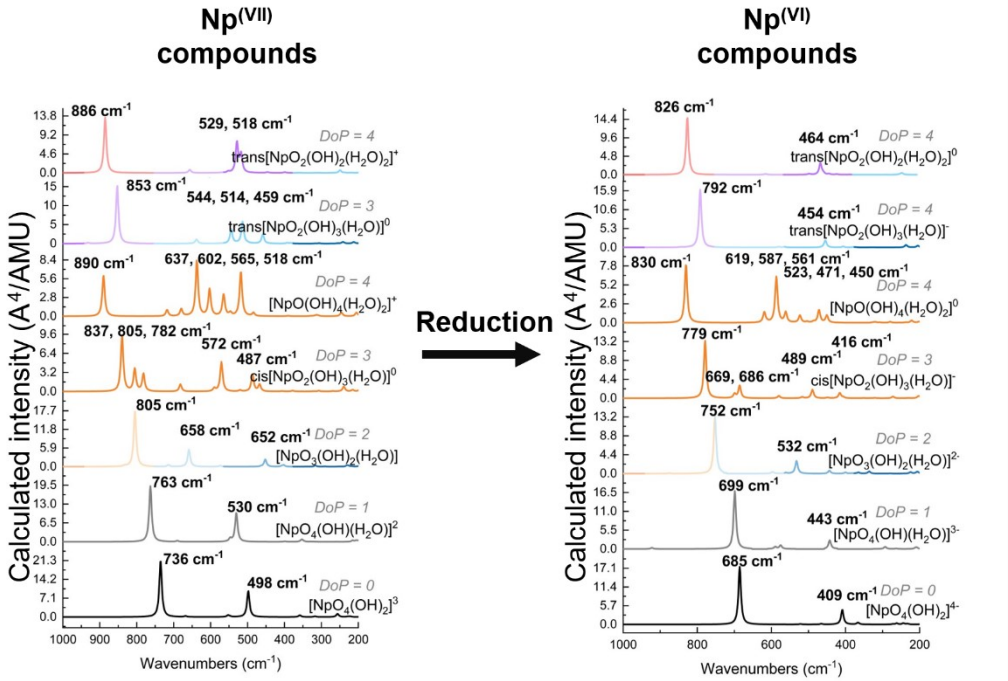

corresponds to the protonation path.

Figure S3: Predicted Raman spectra of Np(VII) and corresponding Np(VI) compounds in protonation path 3 and 4. Here DoP stands for Degree of Protonation. The color of each line corresponds to the protonation path.

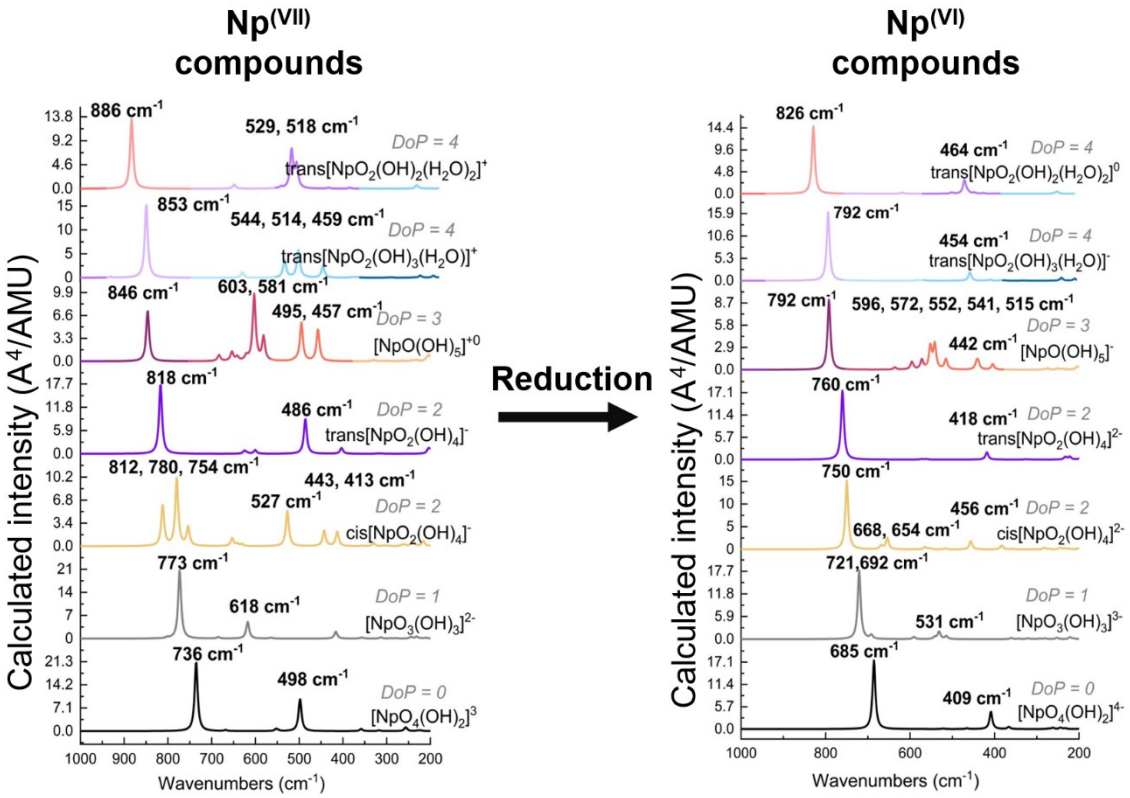

Figure S4: Predicted Raman spectra of Np(VII) and corresponding Np(VI) compounds in protonation path 5 and 6. Here DoP stands for Degree of Protonation. The color of each line corresponds to the protonation path.

1.5 Benchmarking TD-DFT calculations

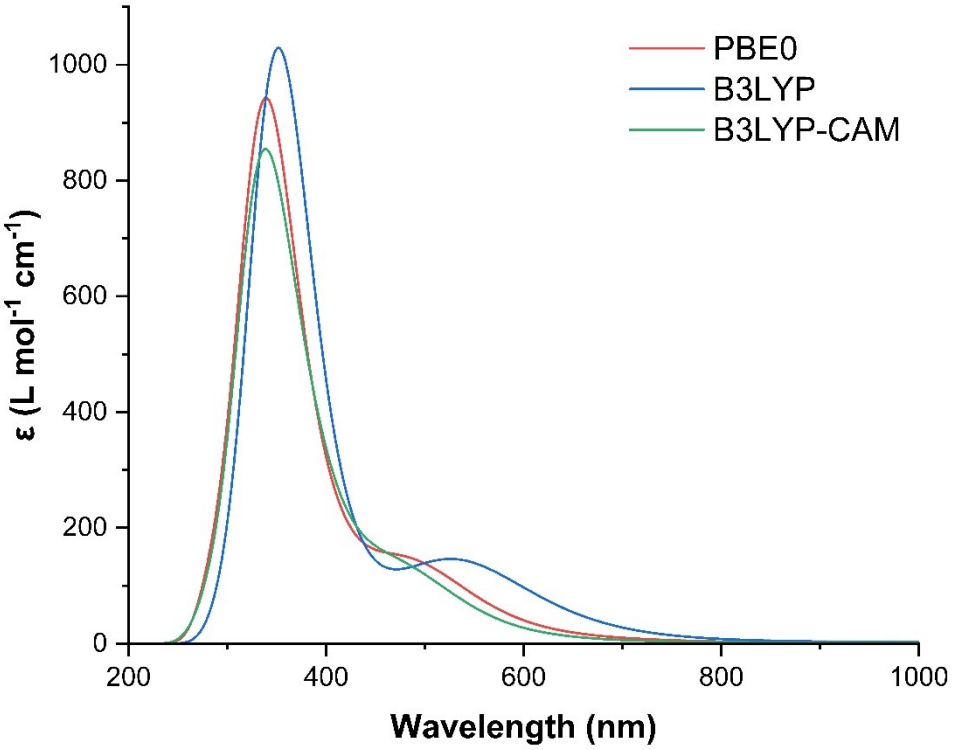

Figure S5: Simulated spectra of $[NpO_4(OH)_2]^{3-}_{(aq)}$ with TD-DFT using different functionals.

1.6 Choice of the functional for DFT calculations

In this study, the B3LYP functional was employed for the computational analysis of actinide systems, with a specific focus on Np(V-VII) compounds. The choice of B3LYP is grounded in its extensive and successful application within the computational chemistry community, particularly for actinide elements. B3LYP has demonstrated consistent accuracy in predicting geometries, electronic structures, bonding characteristics, vibrational spectroscopy, and excited state properties, making it a reliable choice for our investigations.

Previous work within our research group has shown that the B3LYP functional provides excellent agreement with experimental data, particularly when predicting the geometry and Raman features of neptunium compounds across various oxidation states (V-VII). For instance, our studies have confirmed that B3LYP closely matches experimental values, as evidenced by the accurate reproduction of vibrational frequencies and bond distances in these complex systems.[1-5]

The broader applicability of B3LYP within actinide chemistry is also supported by its widespread use in the field. Kovács *et al.* have conducted a comprehensive review of computational methods in actinide chemistry, highlighting that B3LYP is particularly effective for calculating An=O bond distances, vibrational features, dissociation energies, ionization energies, and electronic spectra.[6] Furthermore, numerous studies have successfully utilized B3LYP in

analyzing reaction mechanisms[7, 8] and vibrational spectroscopy[9, 10] of actinide complexes, further validating its robustness.

In the context of TDDFT calculations, which are essential for exploring excited-state properties, Tecmer *et al.* have evaluated the performance of various functionals and concluded that B3LYP is suitable for (semi)quantitative or qualitative analyses.[11] While CAM-B3LYP has been shown to yield optimal results for predicting the UV-Vis spectra of $UO2^{2+}$,[11] our benchmarking study revealed that B3LYP provided the best agreement with experimental observations when simulating the spectra of $[NpO4(OH)2]^{3-}$. Specifically, B3LYP most accurately reproduced the wavelength corresponding to peak maxima, the separation between spectral features, and the overall shape of the spectrum (Figures S5 and S6). This outcome strongly supports our selection of B3LYP for TDDFT calculations in this study. The reliability of B3LYP in predicting electric and magnetic properties of actinide systems is further verified by previous research by Su *et al*.,[12] Gendron *et al*.,[13] Heaven *et al*.,[14] and Hu *et al*.,[15] who have demonstrated its effectiveness across a range of actinide compounds. These findings collectively affirm the robustness and versatility of B3LYP as a functional in the computational study of actinide chemistry.

2. Experimental evidence of Np(VII) protonation

2.1 Titration studies of Np(VII) solutions

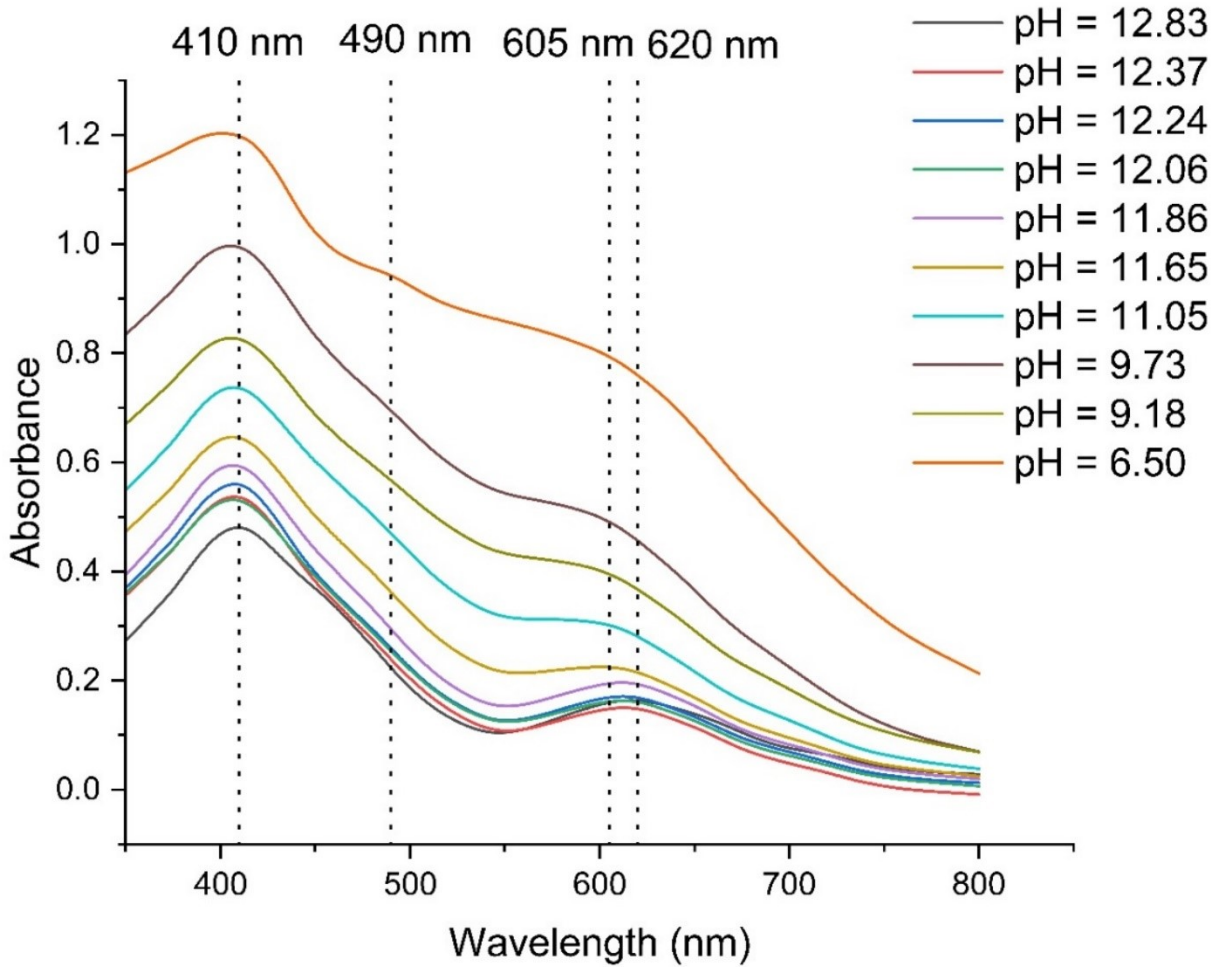

Figure S6: Stacked UV-Vis spectra at each pH value of the titrations. Here 410 nm and 620 nm correspond to the typical absorption bands of $[NpO_4(OH)_2]^{3-}_{(aq)}$.

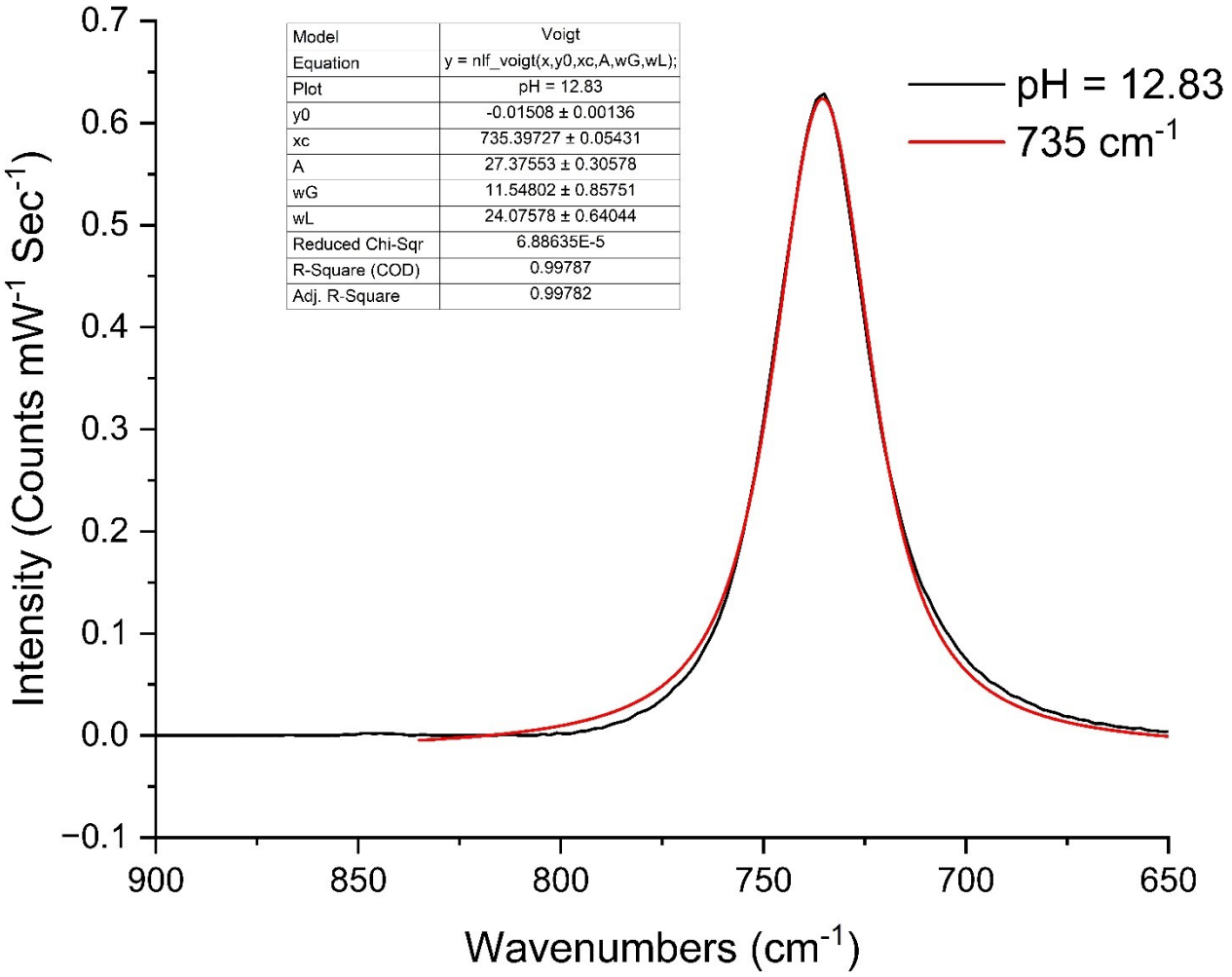

Figure S7: Solution Raman spectra of pH 12.83 solution with fitting parameters in the spectral window of 900-650 cm^{-1}.

Model	Voigt	
Equation	y = nlf_voigt(x,y0,xc,A,wG,wL);	
Plot	Peak1(pH=12.37)	Peak2(pH=12.37)
y0	-0.00651 ± 0.00167	-0.00651 ± 0.00167
xc	746.604 ± 0.1525	736.58038 ± 5.09656
A	16.28301 ± 2.89481	4.90607 ± 2.63874
wG	17.2418 ± 1.35353	30.60594 ± 3.67894
wL	10.28423 ± 0.99617	3.78467E-13 ± 0.03808
Reduced Chi-Sqr	3.99574E-5	
R-Square (COD)	0.99906	
Adj. R-Square	0.99901	

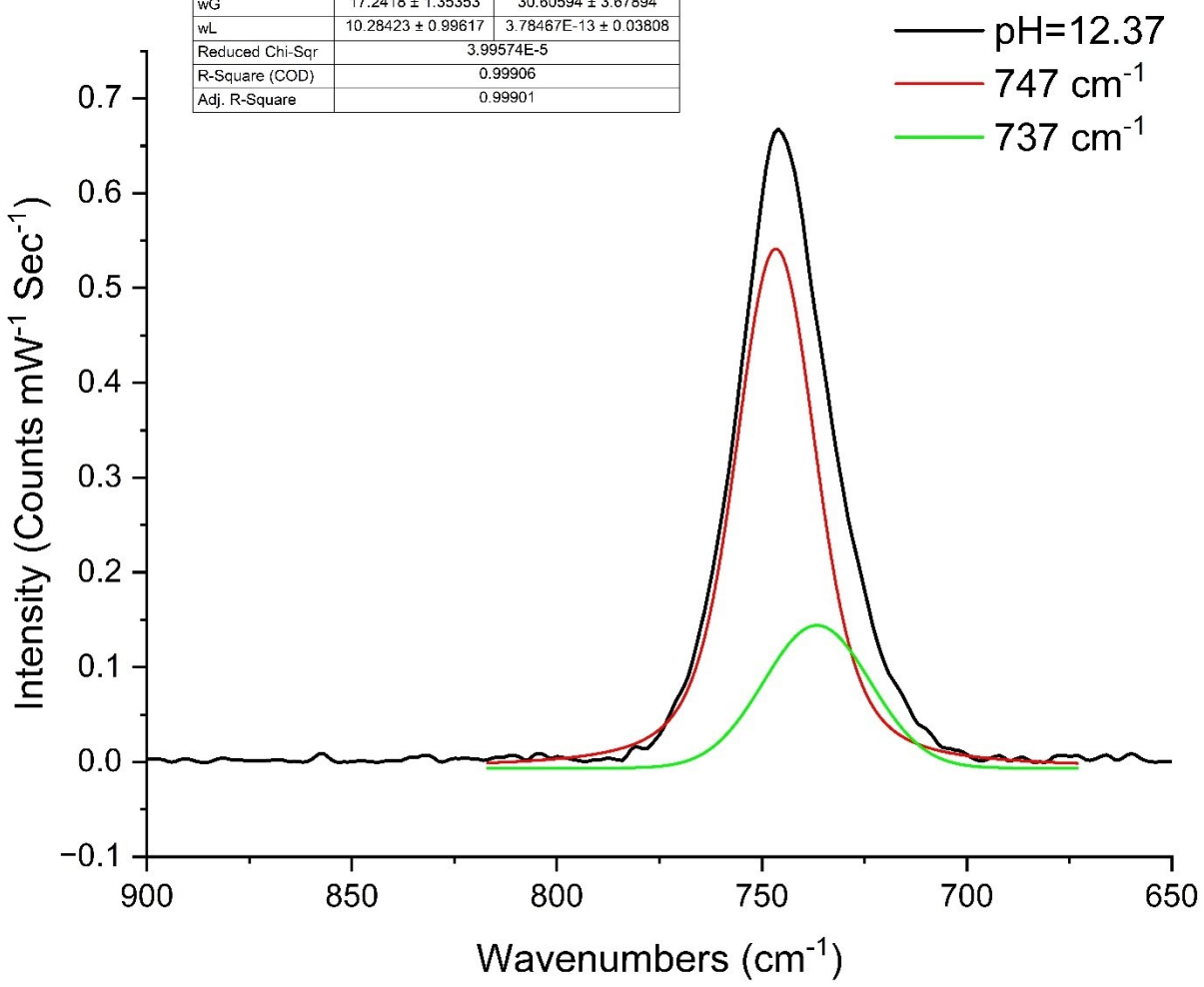

Figure S8: Solution Raman spectra of pH 12.37 solution with fitting parameters in the spectral window of 900-650 cm^{-1}.

Model	Voigt	
Equation	y = nlf_voigt(x,y0,xc,A,wG,wL);	
Plot	Peak1(pH=12.24)	Peak2(pH=12.24)
y0	-0.00262 ± 0.00112	-0.00262 ± 0.00112
xc	746.65593 ± 0.14274	737.4943 ± 2.96071
A	15.01897 ± 2.02943	5.57001 ± 1.83293
wG	17.9539 ± 0.90044	31.32437 ± 2.11998
wL	8.83407 ± 0.69631	6.72123E-14 ± 0.90237
Reduced Chi-Sqr	3.50544E-5	
R-Square (COD)	0.99902	
Adj. R-Square	0.99898	

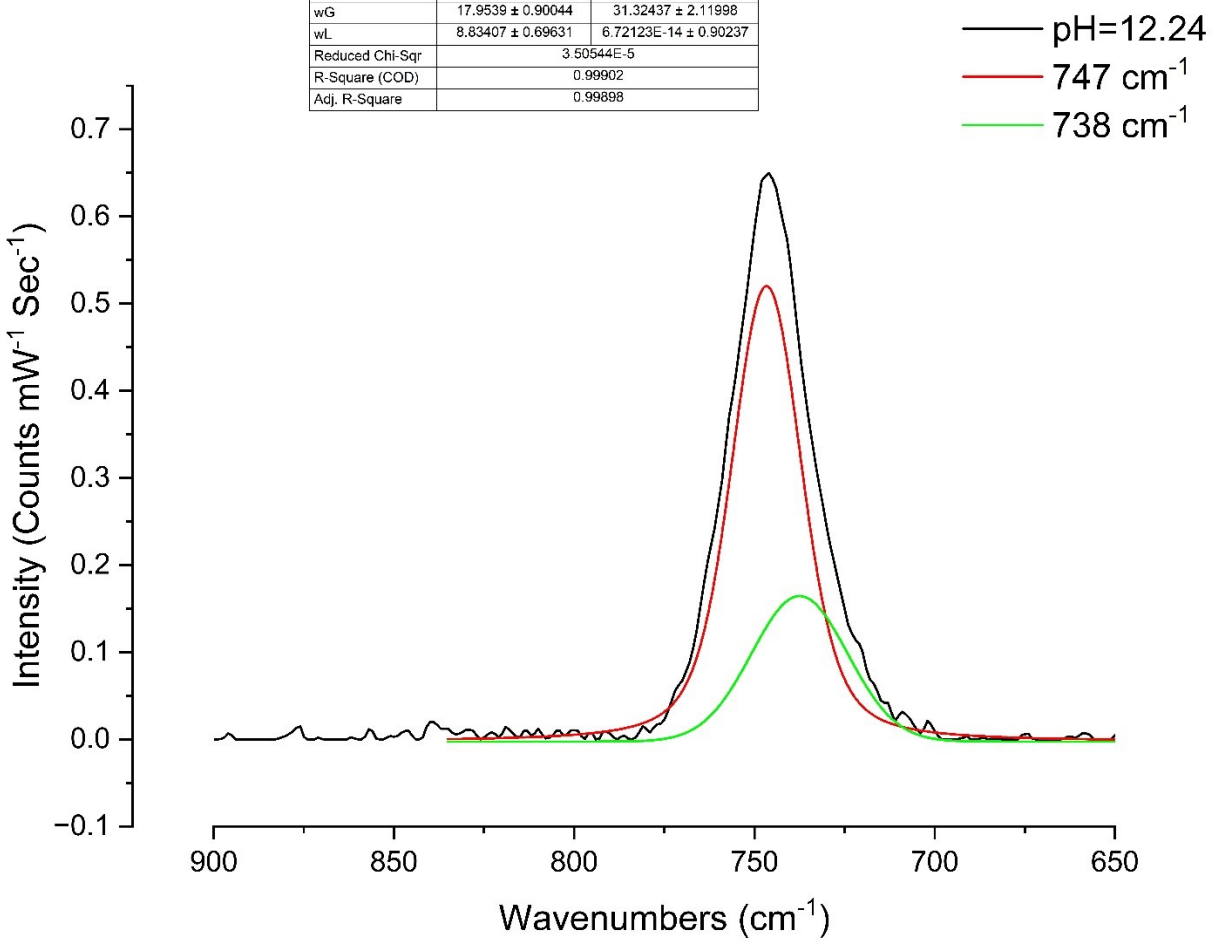

Figure S9: Solution Raman spectra of pH 12.24 solution with fitting parameters in the spectral window of 900-650 cm^{-1}.

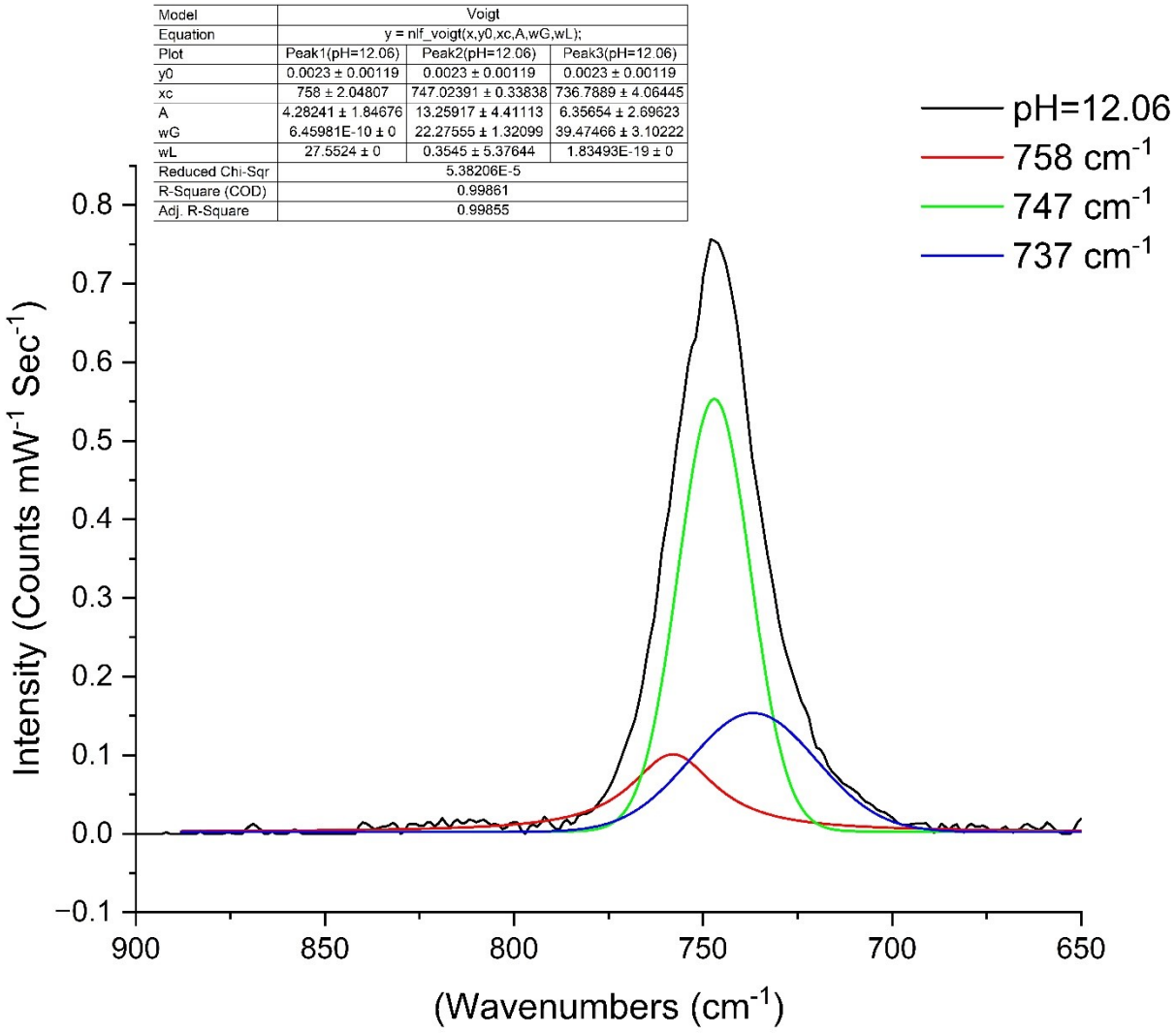

Figure S10: Solution Raman spectra of pH 12.06 solution with fitting parameters in the spectral window of 900-650 cm^{-1}.

Model	Voigt		
Equation	y = nlf_voigt(x,y0,xc,A,wG,wL);		
Plot	Peak1(pH=11.86)	Peak2(pH=11.86)	Peak3(pH=11.86)
y0	-0.00241 ± 0.00186	-0.00241 ± 0.00186	-0.00241 ± 0.00186
xc	754.79969 ± 0.92816	744.19113 ± 0.58032	736.9916 ± 1.28721
A	10.10259 ± 1.51689	11.49912 ± 2.27904	5.13515 ± 0.75047
wG	16.82731 ± 1.63633	6.91071 ± 3.40558	27.84053 ± 0
wL	4.72398 ± 1.66401	15.62987 ± 3.33592	4.46011 ± 0
Reduced Chi-Sqr	5.43295E-5		
R-Square (COD)	0.99909		
Adj. R-Square	0.99903		

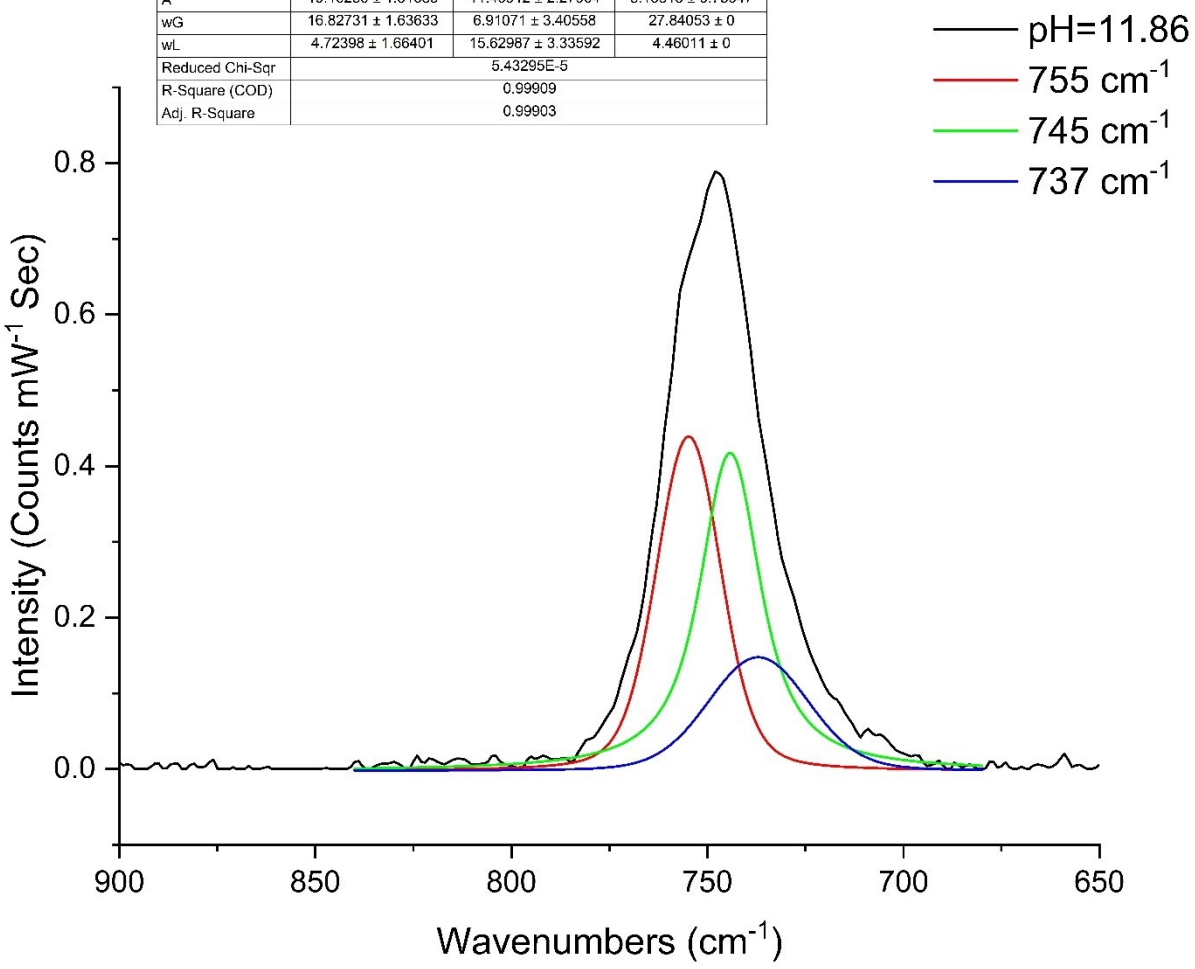

Figure S11: Solution Raman spectra of pH 11.86 solution with fitting parameters in the spectral window of 900-650 cm^{-1}.

Model	Voigt		
Equation	y = nlf_voigt(x,y0,xc,A,wG,wL);		
Plot	Peak1(pH=11.65)	Peak2(pH=11.65)	Peak3(pH=11.65)
y0	-0.00246 ± 0.00163	-0.00246 ± 0.00163	-0.00246 ± 0.00163
xc	757.65438 ± 0.42213	747.24635 ± 0.58149	735.57121 ± 48.90962
A	13.6428 ± 7.82832	14.94967 ± 32.58592	4.50187 ± 24.92327
wG	4.00239E-8 ± 945.80331	13.64801 ± 5.13264	19.98069 ± 44.59426
wL	18.54501 ± 2.35024	11.64492 ± 24.06588	21.58061 ± 9.25952
Reduced Chi-Sqr	3.90843E-5		
R-Square (COD)	0.99941		
Adj. R-Square	0.99937		

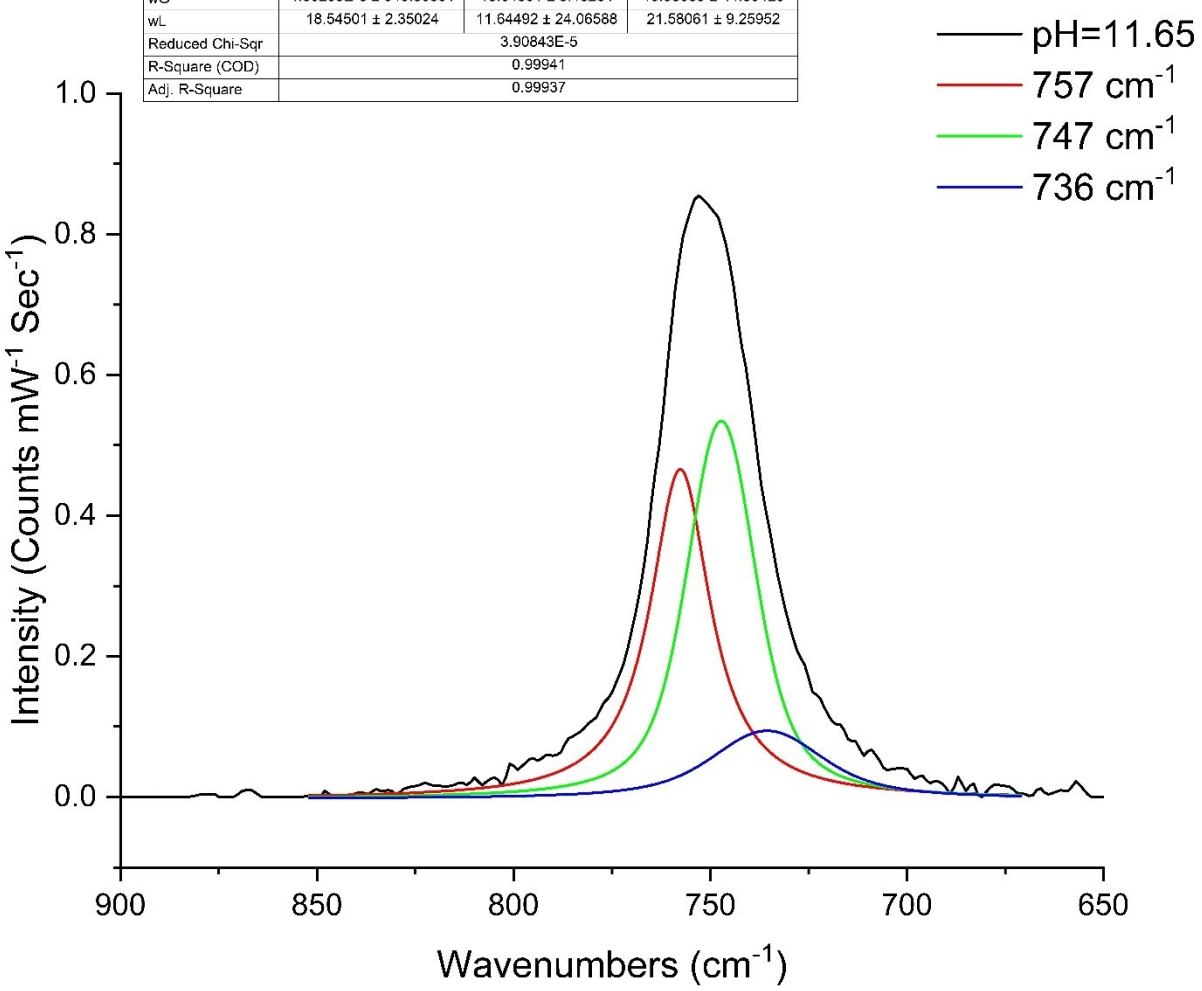

Figure S12: Solution Raman spectra of pH 11.65 solution with fitting parameters in the spectral window of 900-650 cm^{-1}.

Model	Voigt		
Equation	y = nlf_voigt(x,y0,xc,A,wG,wL);		
Plot	Peak1(pH=11.05)	Peak2(pH=11.05)	Peak3(pH=11.05)
y0	-0.02587 ± 0.00262	-0.02587 ± 0.00262	-0.02587 ± 0.00262
xc	790.99259 ± 0	775.01617 ± 0	756.46925 ± 0.19373
A	5.37841 ± 0.8945	10.11224 ± 1.97666	43.62515 ± 1.20791
wG	11.74509 ± 3.93651	25.02043 ± 4.06053	6.29975 ± 1.40687
wL	12.02202 ± 4.78124	3.67811E-13 ± 0.26272	20.93893 ± 0.84038
Reduced Chi-Sqr	2.88069E-4		
R-Square (COD)	0.99804		
Adj. R-Square	0.99794		

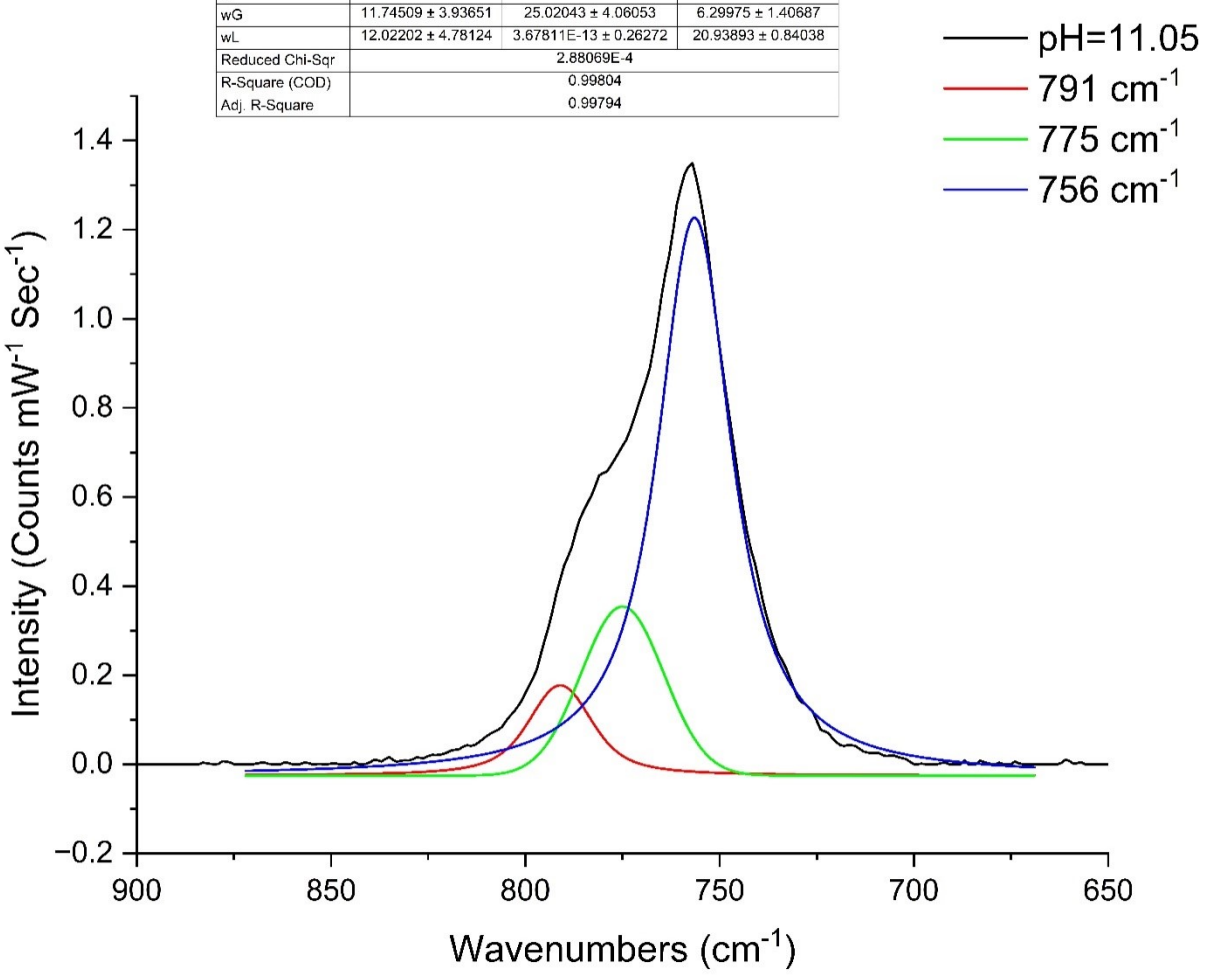

Figure S13: Solution Raman spectra of pH 11.05 solution with fitting parameters in the spectral window of 900-650 cm^{-1}.

Model	Voigt		
Equation	y = nlf_voigt(x,y0,xc,A,wG,wL);		
Plot	Peak1(pH=9.73)	Peak2(pH=9.73)	Peak3(pH=9.73)
y0	-0.02774 ± 0.0018	-0.02774 ± 0.0018	-0.02774 ± 0.0018
xc	793.31446 ± 0.06364	773.57707 ± 1.58562	758.62621 ± 3.39771
A	42.25962 ± 0.61306	47.20997 ± 11.6726	35.51234 ± 12.28796
wG	6.66961 ± 0.74728	25.30614 ± 2.13172	17.78943 ± 3.26465
wL	14.02312 ± 0.6638	6.45044E-44 ± 8.73847E7	17.67611 ± 3.92283
Reduced Chi-Sqr	1.01878E-4		
R-Square (COD)	0.99985		
Adj. R-Square	0.99985		

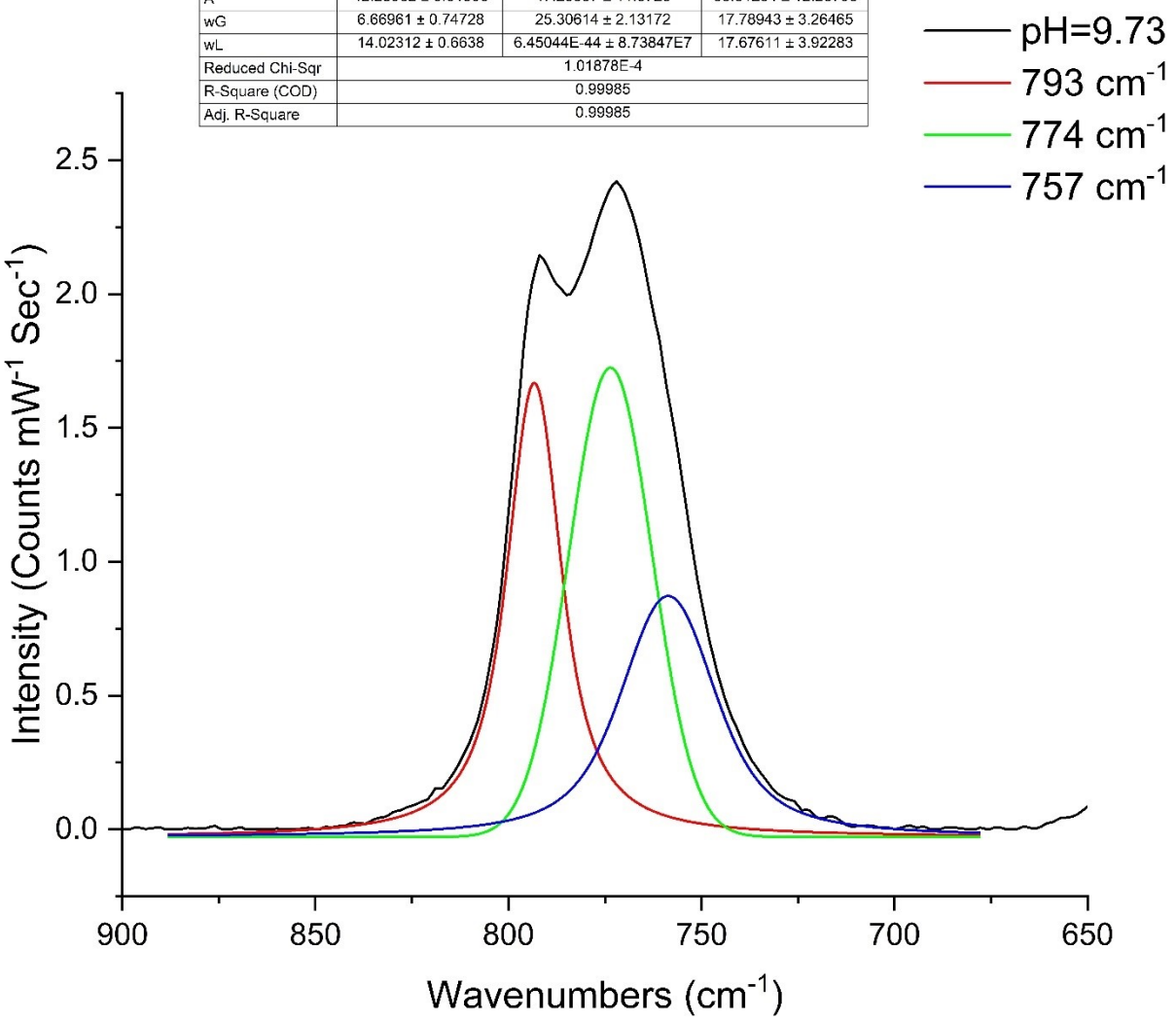

Figure S14: Solution Raman spectra of pH 9.73 solution with fitting parameters in the spectral window of 900-650 cm^{-1}.

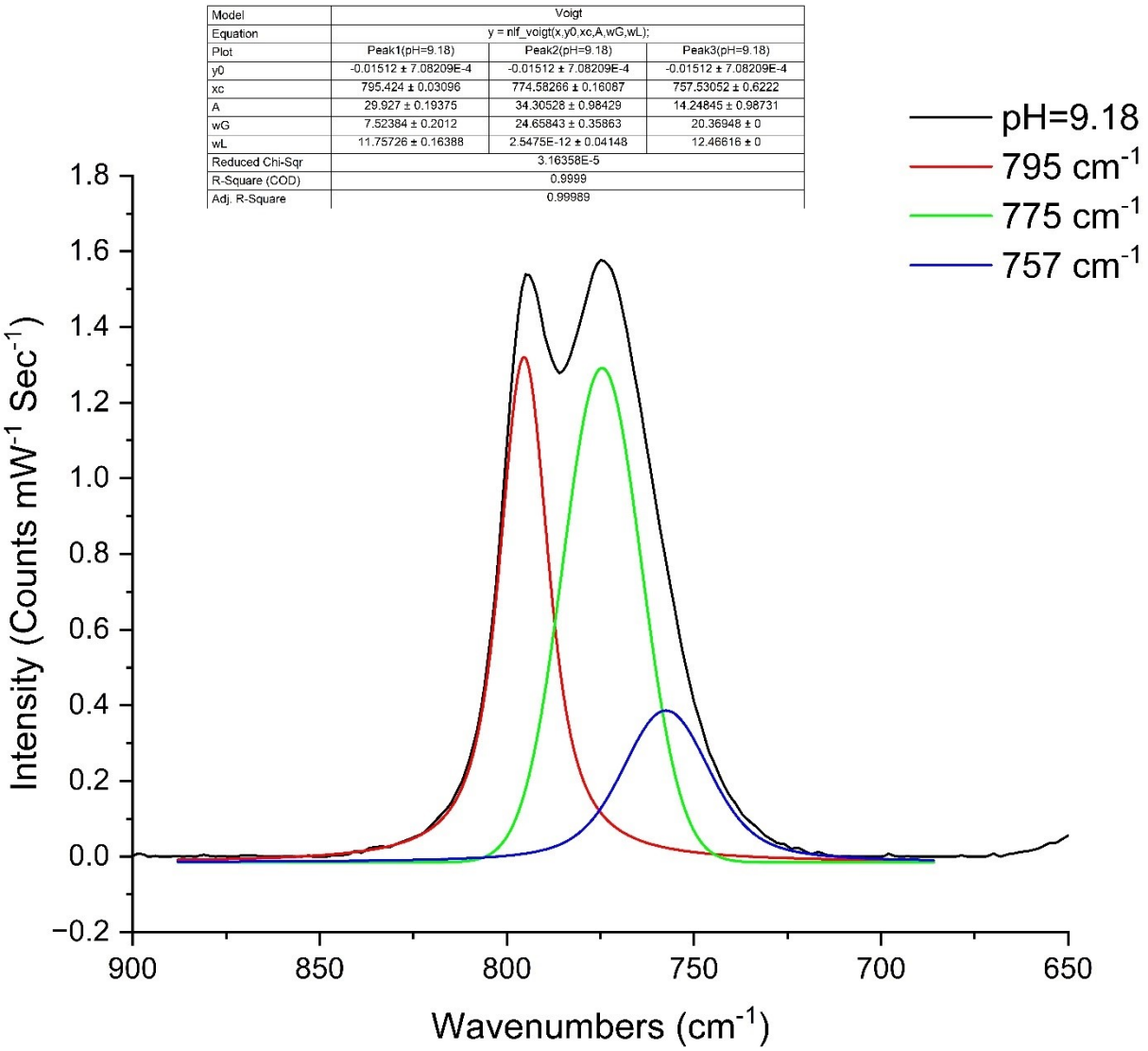

Figure S15: Solution Raman spectra of pH 9.18 solution with fitting parameters in the spectral window of 900-650 cm^{-1} .

Model	Voigt		
Equation	y = nlf_voigt(x,y0,xc,A,wG,wL);		
Plot	Peak1(pH=6.50)	Peak2(pH=6.50)	Peak3(pH=6.50)
y0	-0.02954 ± 0.00185	-0.02954 ± 0.00185	-0.02954 ± 0.00185
xc	799.84271 ± 0.03368	789.71785 ± 0	775.57132 ± 0
A	10.37153 ± 0.14899	38.99292 ± 0.69254	32.72586 ± 0.62665
wG	11.34131 ± 0.10197	30.34078 ± 0.88735	11.8131 ± 1.1237
wL	7.75774E-44 ± 2.47145E7	11.73197 ± 1.30842	25.01176 ± 1.01378
Reduced Chi-Sqr	9.24637E-5		
R-Square (COD)	0.99968		
Adj. R-Square	0.99966		

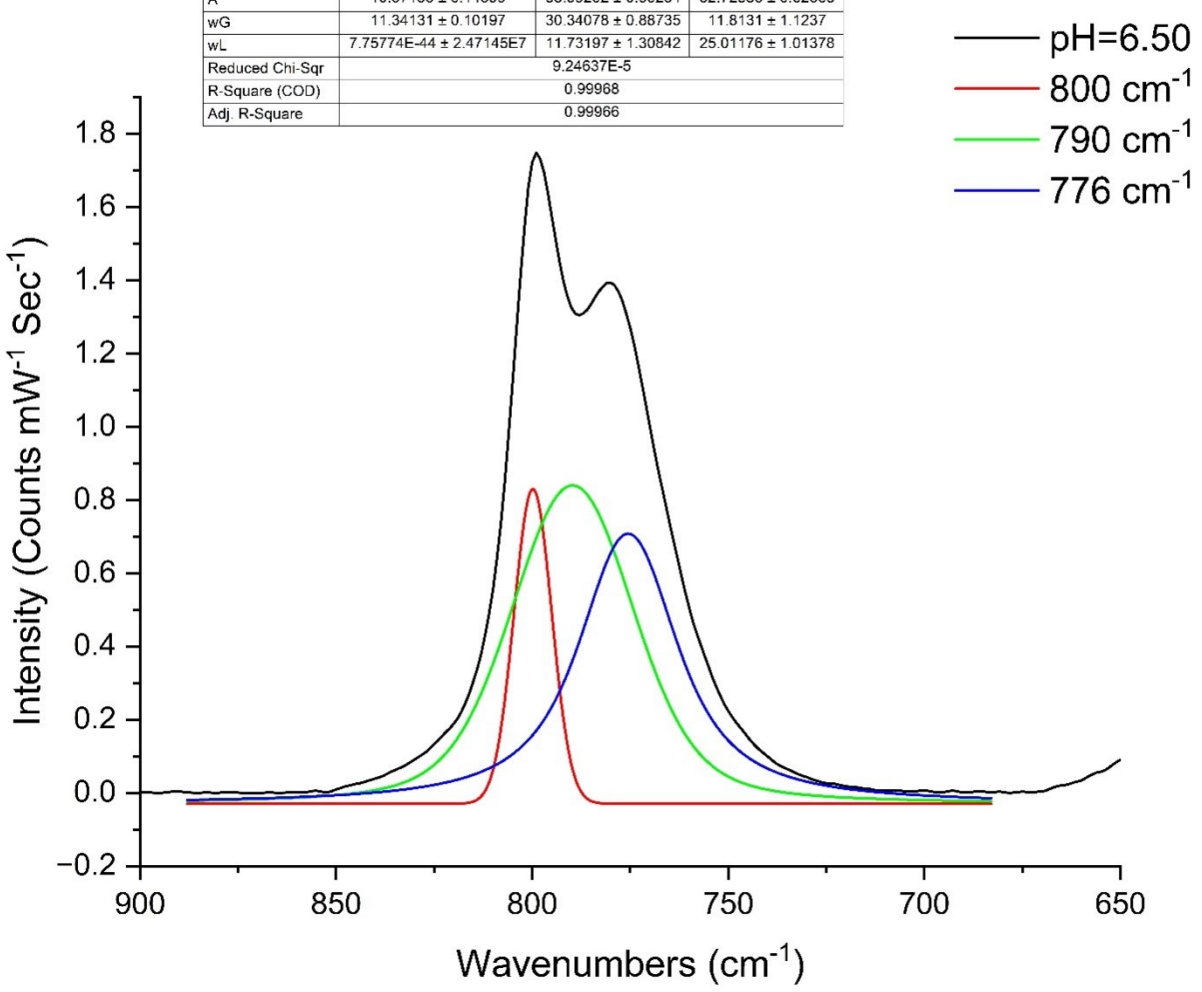

Figure S16: Solution Raman spectra of pH 6.50 solution with fitting parameters in the spectral window of 900-650 cm^{-1}.

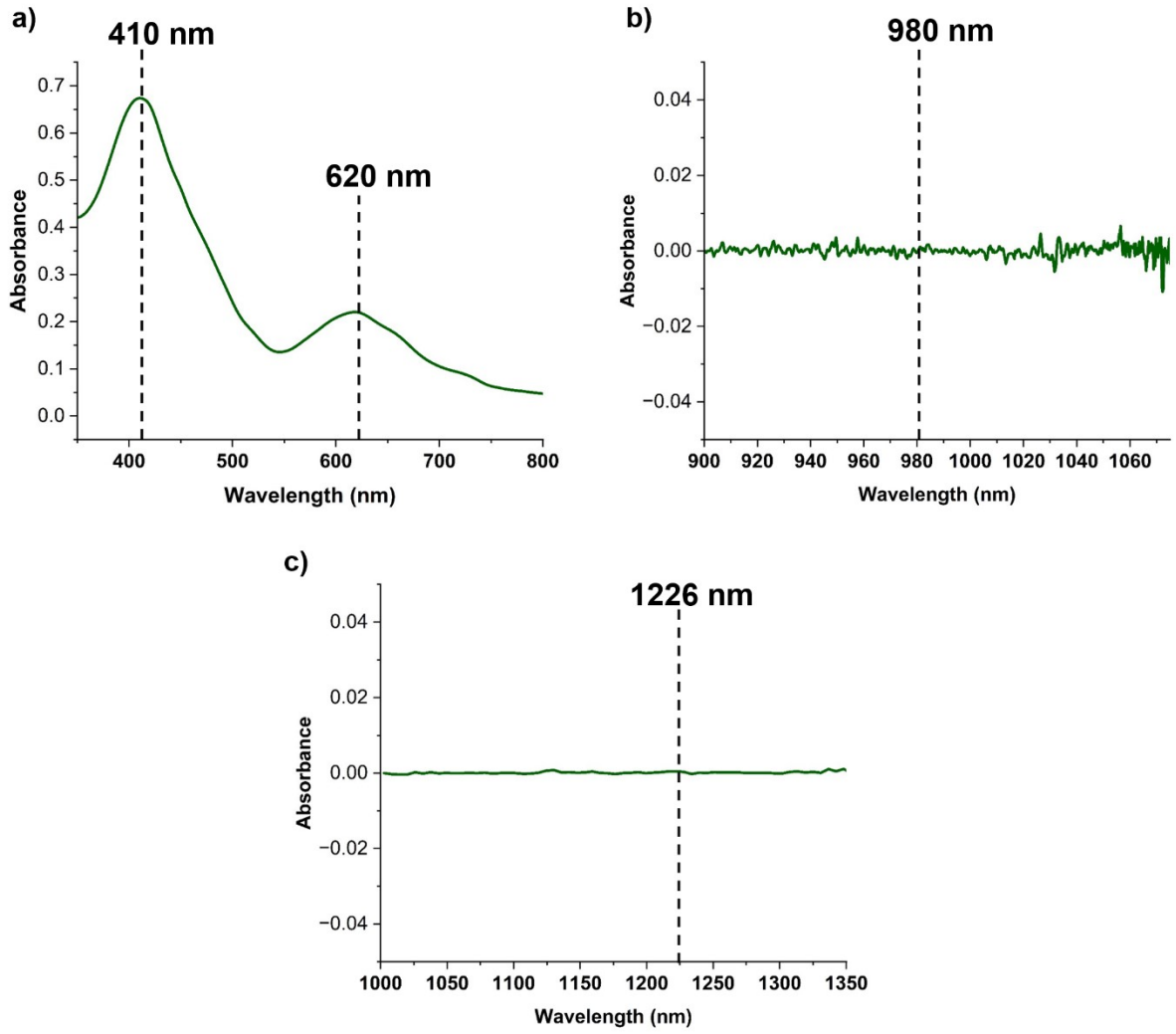

Figure S17: Optical spectroscopy of the solution formed by dissolving the precipitate from pH 6.50 solution in 1M LiOH. Here a), b), and c) are UV-Vis, Vis and NIR spectra respectively.

2.2 Protonation of Np(VII) Solids by Acid Vapor Diffusion

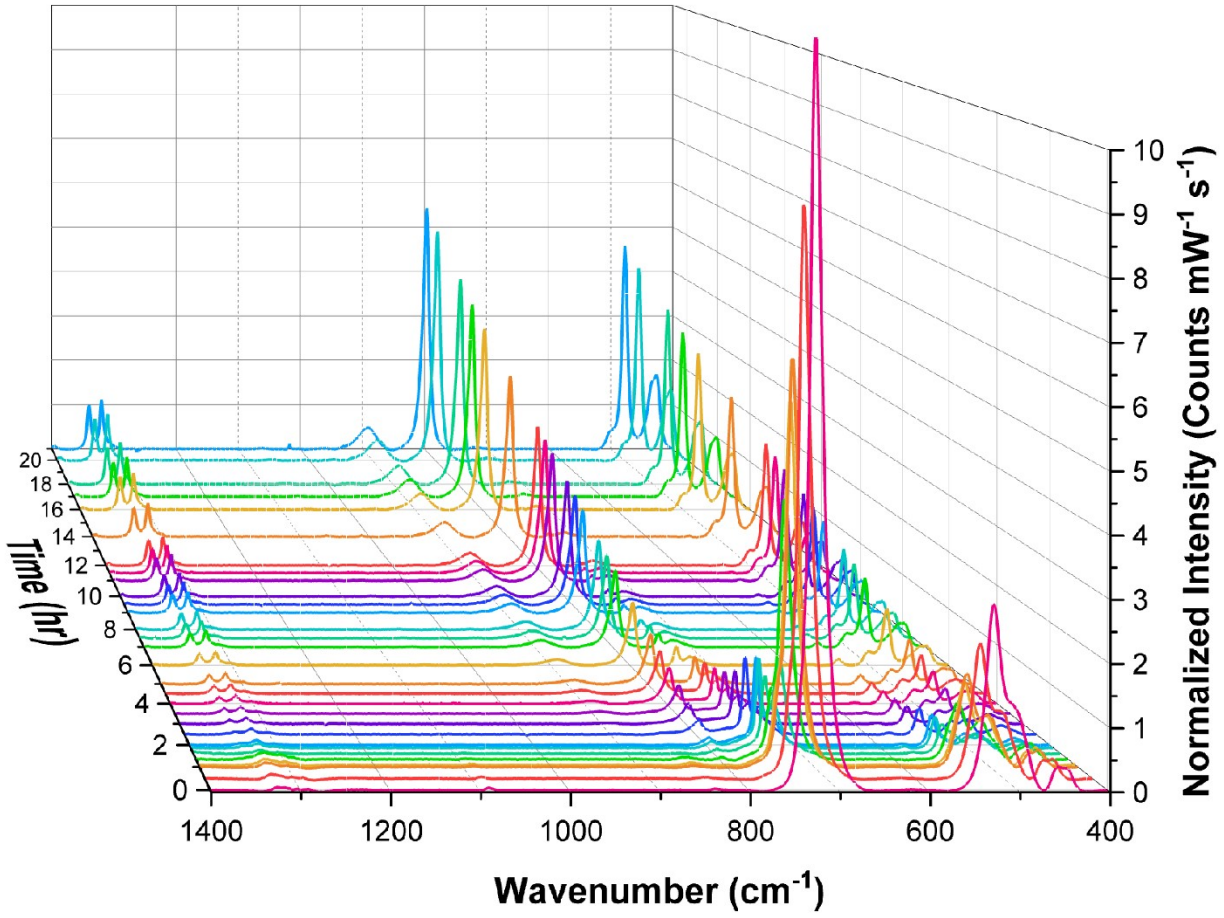

Figure S18: Overlay of solid-state Raman spectra collected on a single sample of $[(Co(NH_3)_6)(NpO_4(OH)_2)]\cdot(H_2O)_n$ (n = 2-4) in the spectral window 1400-400 cm-1. Spectra were collected periodically over the course of 21 hrs while the sample was continuously exposed to acidic vapor.

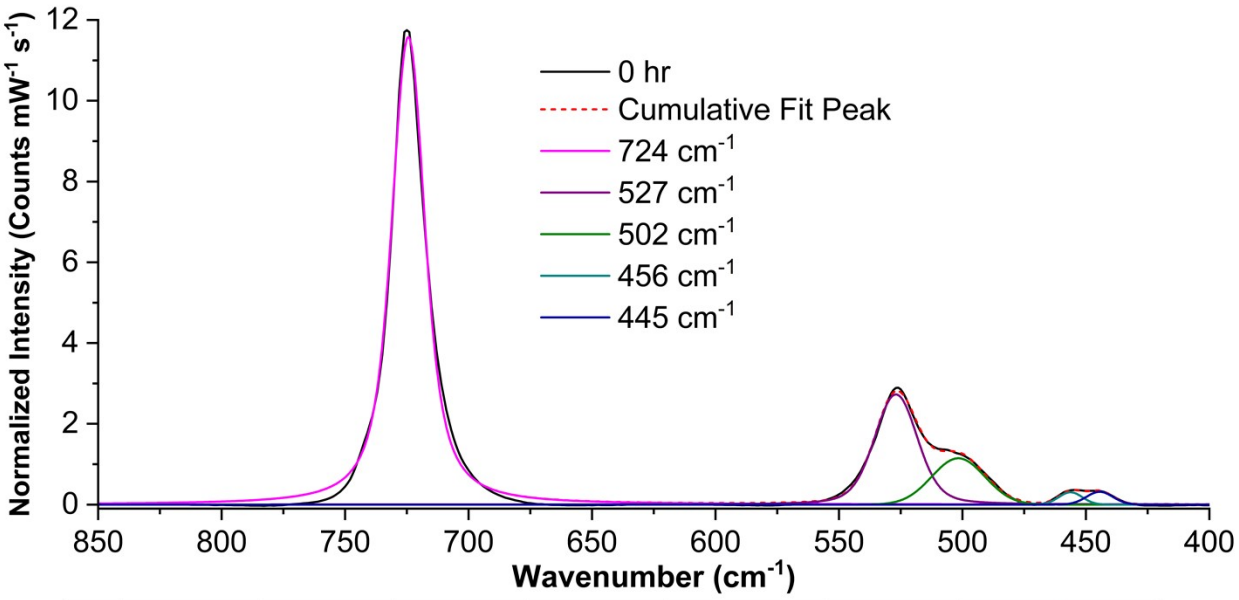

	y0		xc		A		wG		wL		FWHM		Statistics	
	Value	Standard Error	Value	Standard Error	Value	Standard Error	Value	Standard Error	Value	Standard Error	Value	Standard Error	Reduced Chi-Sqr	Adj. R-Square
Peak1()	0	0	724.4	0.03184	257.4	1.467	9.285	0.282	10.49	0.2412	16.1	0.1099	0.01477	0.9958
Peak2()	0	0	526.9	0.3234	67.01	3.023	17.25	1.385	5.828	1.682	20.58	0.66		
Peak3()	0	0	501.7	0.8431	30.88	2.495	25.28	1.874	3.595E-24	--	25.28	1.874		
Peak4()	0	0	456.2	3.437	3.656	3.041	11.21	10.27	3.89E-8	13.38	11.21	5.202		
Peak5()	0	0	444.5	3.932	4.275	2.831	12.65	6.024	1E-18	0	12.65	6.024		

Figure S19: Solid-state Raman spectra with fitting parameters and statistics of neat

$[(Co(NH_3)_6)(NpO_4(OH)_2)]\cdot(H_2O)_n$ (n = 2-4).

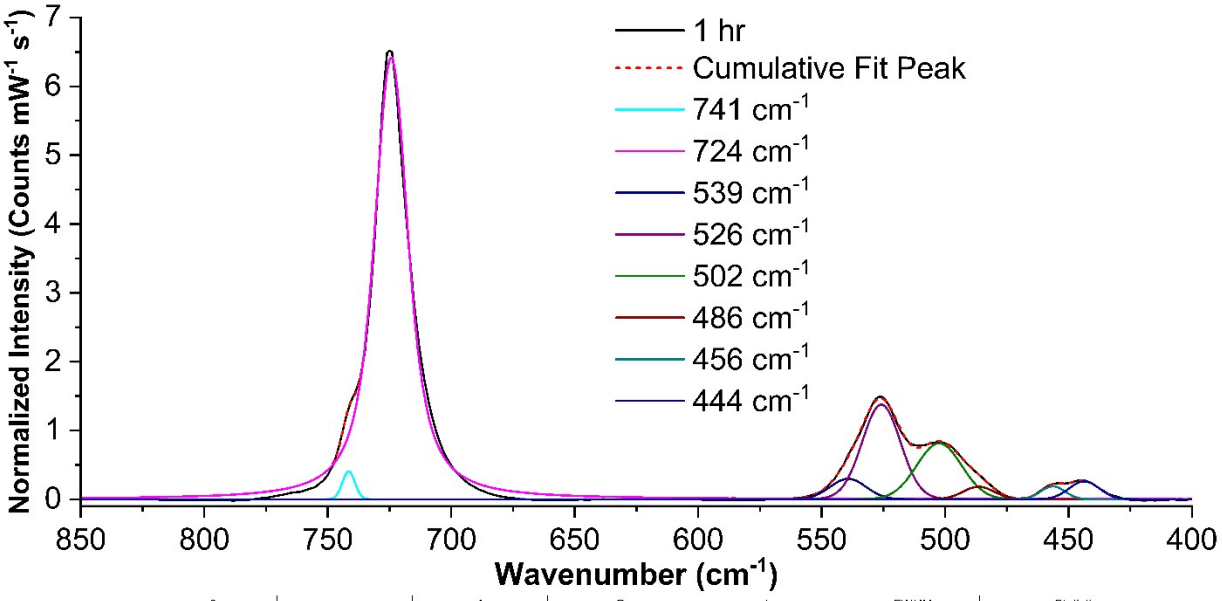

	y0		xc		A		wG		wL		FWHM		Statistics	
	Value	Standard Error	Value	Standard Error	Value	Standard Error	Value	Standard Error	Value	Standard Error	Value	Standard Error	Reduced Chi-Sqr	Adj. R-Square
Peak1(1 hr)	0	0	741.5	0.2774	2.583	0.7524	5.964	2.301	8.826E-10	3.674	5.964	0.7334	0.00418	0.9962
Peak2(1 hr)	0	0	724.3	0.03822	148.7	1.239	8.297	0.3287	11.84	0.2893	16.29	0.1202		
Peak3(1 hr)	0	0	539.3	18.41	5.434	17.43	17.14	28.73	6.071E-8	41.44	17.14	13.4		
Peak4(1 hr)	0	0	525.8	3.941	27.12	29.3	17.95	13.3	0.5947	23.86	18.27	7.736		
Peak5(1 hr)	0	0	502.4	2.421	18.5	21.9	21.37	11.27	1.521E-4	17.54	21.37	14.18		
Peak6(1 hr)	0	0	486.4	7.741	2.891	9.138	14.77	12.37	1.236E-19	--	14.77	12.37		
Peak7(1 hr)	0	0	456.4	2.724	2.315	1.704	11.53	4.868	4.39E-20	--	11.53	4.868		
Peak8(1 hr)	0	0	443.7	2.666	3.995	1.549	14.4	4.229	5.438E-16	0	14.4	4.229		

Figure S20: Solid-state Raman spectra with fitting parameters and statistics of $[(Co(NH_3)_6)(NpO_4(OH)_2)]\cdot(H_2O)_n$ (n = 2-4) after 1 hour of exposure to acidic vapor.

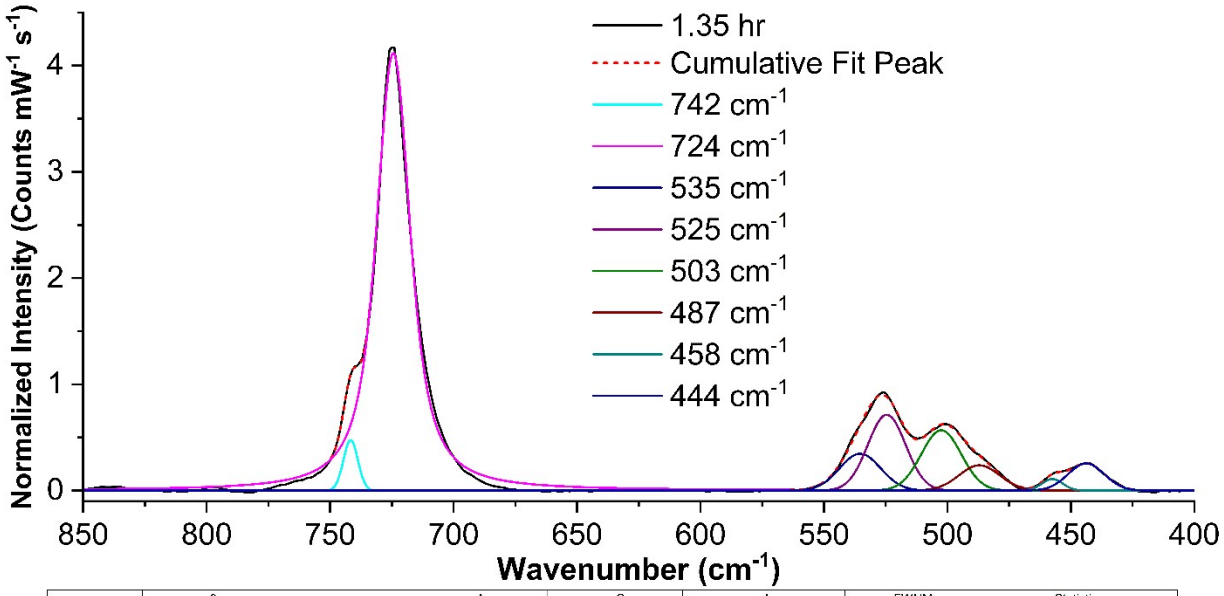

	y0		xc		A		wG		wL		FWHM		Statistics	
	Value	Standard Error	Value	Standard Error	Value	Standard Error	Value	Standard Error	Value	Standard Error	Value	Standard Error	Reduced Chi-Sqr	Adj. R-Square
Peak1(1.35 hr)	0	0	741.7	0.1567	3.495	0.5187	6.888	1.299	1.177E-9	2.11	6.888	0.4088	0.00152	0.9967
Peak2(1.35 hr)	0	0	724.4	0.03785	96.92	0.7876	8.057	0.3209	12.26	0.2759	16.43	0.1169		
Peak3(1.35 hr)	0	0	535.4	39.21	7.222	39.05	19.56	35.69	3.634E-10	28.06	19.56	35.69		
Peak4(1.35 hr)	0	0	524.6	12.83	13.66	39.6	17.98	19.49	0.00418	28.63	17.99	10.39		
Peak5(1.35 hr)	0	0	502.5	3.708	11.49	9.731	19.02	8.604	2.333E-20	--	19.02	8.604		
Peak6(1.35 hr)	0	0	487.1	10.79	4.907	7.825	19.38	9.636	6.017E-29	--	19.38	9.636		
Peak7(1.35 hr)	0	0	457.5	1.47	1.153	0.6359	9.898	3.184	1.776E-13	0.3887	9.898	3.184		
Peak8(1.35 hr)	0	0	443.8	1.184	4.685	0.6917	17.23	2.393	1E-18	0	17.23	2.393		

Figure S21: Solid-state Raman spectra with fitting parameters and statistics of $[(Co(NH_3)_6)(NpO_4(OH)_2)]\cdot(H_2O)_n$ (n = 2-4) after 1.35 hour of exposure to acidic vapor.

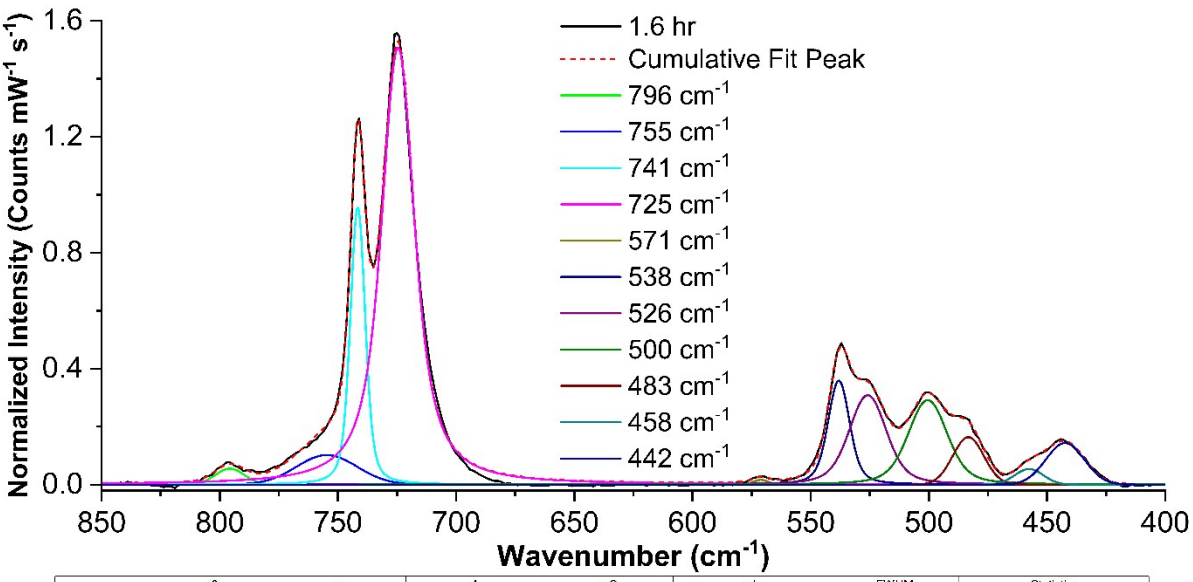

	y0		xc		A		wG		wL		FWHM		Statistics	
	Value	Standard Error	Value	Standard Error	Value	Standard Error	Value	Standard Error	Value	Standard Error	Value	Standard Error	Reduced Chi-Sqr	Adj. R-Square
Peak1(1.6 hr)	0	0	795.7	0.8945	0.8555	0.6341	14.53	7.247	1.565E-8	14.97	14.53	2.54	1.875E-4	0.9978
Peak2(1.6 hr)	0	0	754.7	4.594	3.314	1.755	30	21.23	0.4908	33.62	30.26	6.849		
Peak3(1.6 hr)	0	0	741.6	0.03205	8.892	1.346	5.802	0.7155	2.863	1.384	7.483	0.2461		
Peak4(1.6 hr)	0	0	724.6	0.05299	36.01	1.01	8.396	0.5816	12.31	0.6667	16.74	0.1592		
Peak5(1.6 hr)	0	0	571.1	1.535	0.1308	0.07052	7.314	3.964	6.529E-22	4.768E7	7.314	3.964		
Peak6(1.6 hr)	0	0	538.1	0.2821	4.821	2.011	8.361	2.267	4.156	4.535	10.8	1.048		
Peak7(1.6 hr)	0	0	525.9	0.7462	7.134	4.924	14.6	5.642	6.962	13.57	18.68	4.513		
Peak8(1.6 hr)	0	0	500.5	0.6932	7.051	4.874	15.34	7.871	7.236	18.32	19.57	4.783		
Peak9(1.6 hr)	0	0	483.3	1.041	2.707	1.348	15.51	2.545	3.403E-22	--	15.51	2.545		
Peak10(1.6 hr)	0	0	457.6	2.647	0.8235	0.5535	14.31	4.683	2.802E-19	--	14.31	4.683		
Peak11(1.6 hr)	0	0	442.4	1.5	2.921	0.5111	19.09	2.278	1E-18	0	19.09	2.278		

Figure S22: Solid-state Raman spectra with fitting parameters and statistics of $[(Co(NH_3)_6)(NpO_4(OH)_2)]\cdot(H_2O)_n$ (n = 2-4) after 1.6 hour of exposure to acidic vapor.

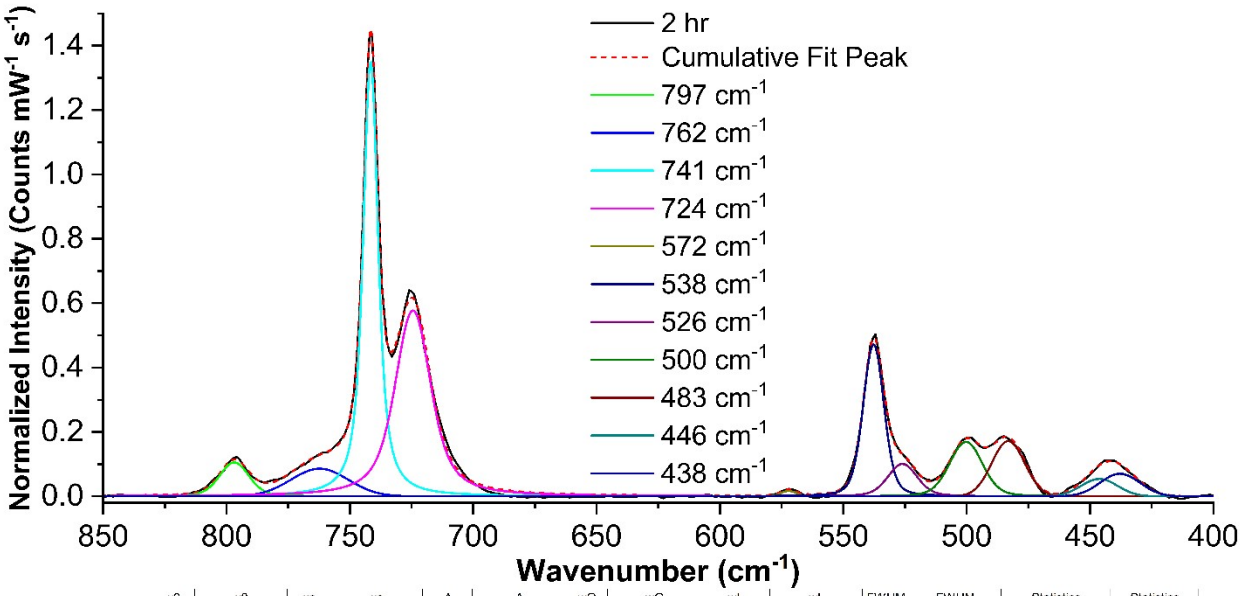

	y0 Value	y0 Standard Error	xc Value	xc Standard Error	A Value	A Standard Error	wG Value	wG Standard Error	wL Value	wL Standard Error	FWHM Value	FWHM Standard Error	Statistics Reduced Chi-Sqr	Statistics Adj. R-Square
Peak1(2 hr)	0	0	796.9	0.2259	1.782	0.1295	11.91	1.812	3.952	2.442	14.17	0.6185	6.217E-5	0.9984
Peak2(2 hr)	0	0	762.3	0.7328	2.502	0.1953	27.27	1.886	2.511E-13	2.216	27.27	1.886		
Peak3(2 hr)	0	0	741.6	0.01368	13.77	0.2919	3.789	0.226	5.118	0.2528	7.212	0.04922		
Peak4(2 hr)	0	0	724.5	0.06597	13.42	0.1915	10.79	0.4397	10.18	0.4454	17.23	0.1935		
Peak5(2 hr)	0	0	572.2	0.8767	0.1354	0.03614	7.456	2.155	1.872E-15	--	7.456	2.155		
Peak6(2 hr)	0	0	537.7	0.1095	5.558	0.7848	8.431	0.7849	2.645	1.507	9.935	0.2841		
Peak7(2 hr)	0	0	526	0.6701	1.712	1.905	11.61	11.14	4.315	22.73	14.09	3.898		
Peak8(2 hr)	0	0	500.3	0.4066	3.082	1.834	13.81	6.159	3.332	14.19	15.68	2.556		
Peak9(2 hr)	0	0	483.2	0.5561	2.874	0.5939	15.71	1.161	1.279E-18	1.385E9	15.71	1.161		
Peak10(2 hr)	0	0	446.2	22.28	1.004	7.814	17.33	12.49	1.795E-20	3.196E14	17.33	12.49		
Peak11(2 hr)	0	0	437.9	29.6	1.42	7.784	18.94	16.22	1.887E-17	0	18.94	16.22		

Figure S23: Solid-state Raman spectra with fitting parameters and statistics of $[(Co(NH_3)_6)(NpO_4(OH)_2)]\cdot(H_2O)_n$ (n = 2-4) after 2.0 hour of exposure to acidic vapor.

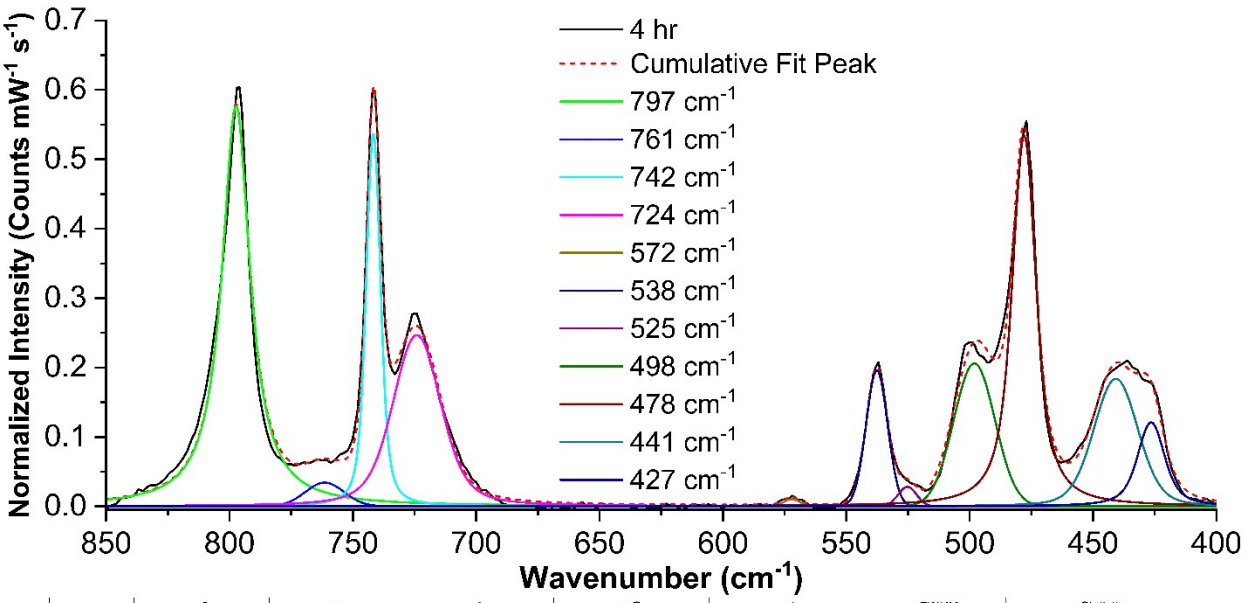

	y0		xc		A		wG		wL		FWHM		Statistics	
	Value	Standard Error	Value	Standard Error	Value	Standard Error	Value	Standard Error	Value	Standard Error	Value	Standard Error	Reduced Chi-Sqr	Adj. R-Square
Peak1(4 hr)	0	0	797.4	0.07103	12.48	0.2057	2.376E-7	11120	13.77	0.2572	13.77	0.2572	1.425E-4	0.9917
Peak2(4 hr)	0	0	761.4	1.598	0.675	0.4191	18.53	15.2	4.869E-5	25.48	18.53	4.13		
Peak3(4 hr)	0	0	741.7	0.05031	4.732	0.3722	5.078	0.665	3.072	0.9631	6.918	0.1517		
Peak4(4 hr)	0	0	724.1	0.3666	7.034	0.359	17.88	1.749	8.705	1.951	22.99	0.8995		
Peak5(4 hr)	0	0	572.1	2.224	0.08548	0.05052	7.759	5.282	5.273E-29	--	7.759	5.282		
Peak6(4 hr)	0	0	537.6	0.2133	2.14	0.1297	10.26	0.5086	1.215E-23	--	10.26	0.5086		
Peak7(4 hr)	0	0	525.3	1.359	0.2642	0.2502	8.78	10.53	9.381E-10	18.09	8.78	3.107		
Peak8(4 hr)	0	0	498.1	0.3446	4.304	0.2657	19.62	0.9619	2.599E-34	1.637E8	19.62	0.9619		
Peak9(4 hr)	0	0	477.9	0.0856	8.818	0.676	6.05	1.303	8.357	1.508	11.66	0.282		
Peak10(4 hr)	0	0	440.8	0.8971	4.543	1.224	18.49	6.597	4.795	10.2	21.18	1.802		
Peak11(4 hr)	0	0	426.5	0.7271	2.114	0.7498	8.301	5.129	7.497	6.835	13.01	1.578		

Figure S24: Solid-state Raman spectra with fitting parameters and statistics of $[(Co(NH_3)_6)(NpO_4(OH)_2)]\cdot(H_2O)_n$ (n = 2-4) after 4 hours of exposure to acidic vapor.

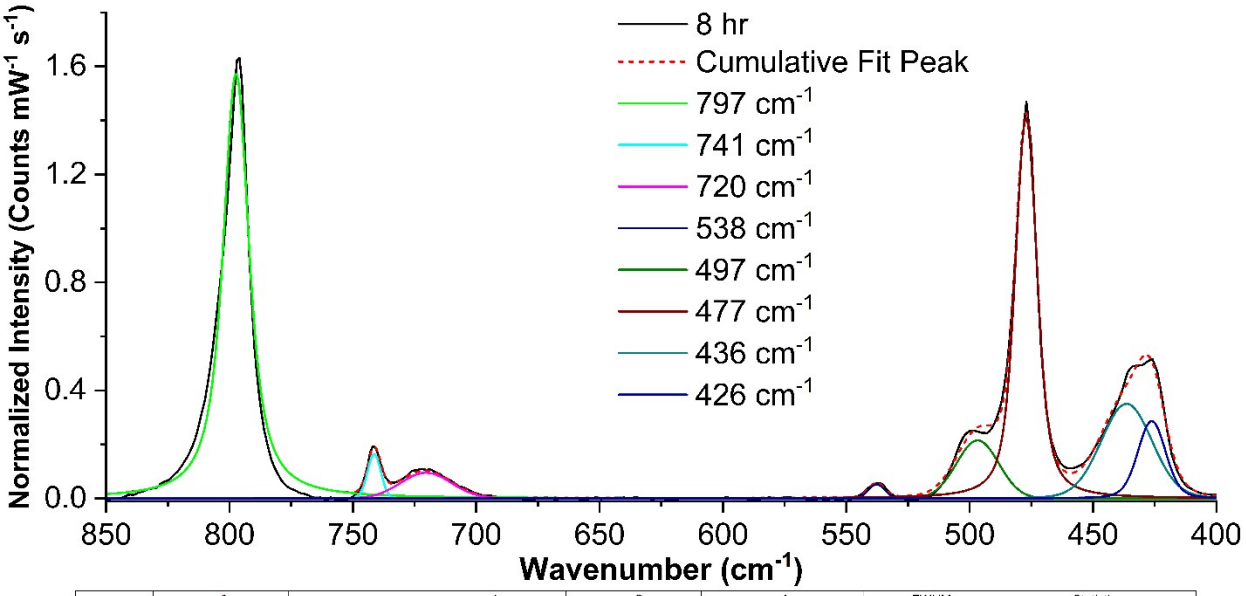

	y0		xc		A		wG		wL		FWHM		Statistics	
	Value	Standard Error	Value	Standard Error	Value	Standard Error	Value	Standard Error	Value	Standard Error	Value	Standard Error	Reduced Chi-Sqr	Adj. R-Square
Peak1(8 hr)	0	0	797.4	0.05083	28.67	0.3176	5.581	0.5387	9.885	0.3657	12.52	0.1861	8.563E-4	0.9899
Peak2(8 hr)	0	0	741.4	0.3234	1.118	0.1488	6.388	0.8236	2.11E-34	--	6.388	0.8236		
Peak3(8 hr)	0	0	720.4	1.173	2.456	0.2538	24.19	3.093	1.178E-20	3.126E7	24.19	3.093		
Peak4(8 hr)	0	0	537.7	1.093	0.4386	0.2443	7.88	6.781	9.932E-12	9.558	7.88	2.883		
Peak5(8 hr)	0	0	496.8	0.7696	4.61	0.7966	20.1	4.39	4.541E-11	6.596	20.1	1.759		
Peak6(8 hr)	0	0	477.1	0.06912	19.48	1.166	7.225	0.8105	5.434	1.12	10.56	0.1926		
Peak7(8 hr)	0	0	436.4	5.911	9.465	7.056	23.08	8.987	2.372	11.42	24.38	6.595		
Peak8(8 hr)	0	0	426.2	0.6868	4.441	6.968	11.57	4.297	3.023	12.03	13.27	5.143		

Figure S25: Solid-state Raman spectra with fitting parameters and statistics of $[(Co(NH_3)_6)(NpO_4(OH)_2)]\cdot(H_2O)_n$ (n = 2-4) after 8 hours of exposure to acidic vapor.

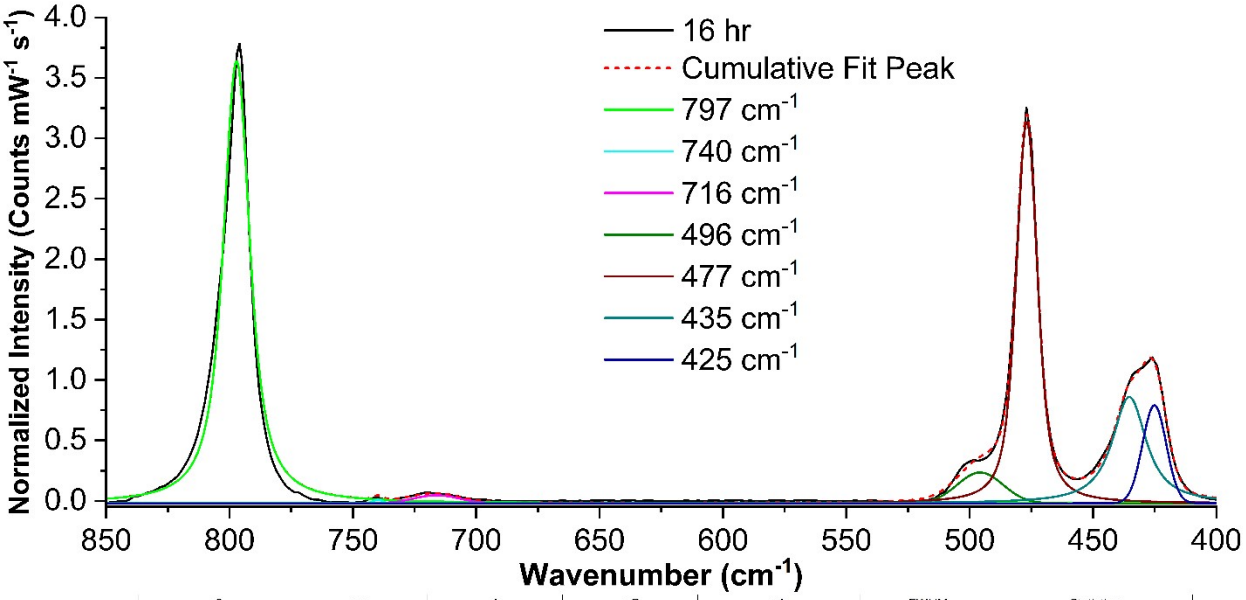

	y0		xc		A		wG		wL		FWHM		Statistics	
	Value	Standard Error	Value	Standard Error	Value	Standard Error	Value	Standard Error	Value	Standard Error	Value	Standard Error	Reduced Chi-Sqr	Adj. R-Square
Peak1(16 hr)	-0.02188	0.00533	797.2	0.04631	67.97	0.8339	5.718	0.5224	10.05	0.3756	12.76	0.1695	0.00378	0.9915
Peak2(16 hr)	-0.02188	0.00533	739.9	3.039	0.15	0.4746	4.62	22.94	6.404E-7	34.26	4.62	8.284		
Peak3(16 hr)	-0.02188	0.00533	716.1	3.223	1.575	0.7635	21.94	13.9	6.504E-12	20.94	21.94	8.072		
Peak4(16 hr)	-0.02188	0.00533	495.8	1.357	5.947	1.757	21.8	7.522	6.471E-9	11.86	21.8	7.527		
Peak5(16 hr)	-0.02188	0.00533	476.8	0.0853	43.09	1.628	6.709	0.5705	5.696	0.6901	10.26	0.1733		
Peak6(16 hr)	-0.02188	0.00533	435.3	1.831	22.14	4.385	4.628	9.003	15.06	3.614	16.45	2.3		
Peak7(16 hr)	-0.02188	0.00533	425.1	1.034	9.856	4.009	11.3	2.236	0.1022	3.239	11.36	1.777		

Figure S26: Solid-state Raman spectra with fitting parameters and statistics of $[(Co(NH_3)_6)(NpO_4(OH)_2)]\cdot(H_2O)_n$ (n = 2-4) after 16 hours of exposure to acidic vapor.

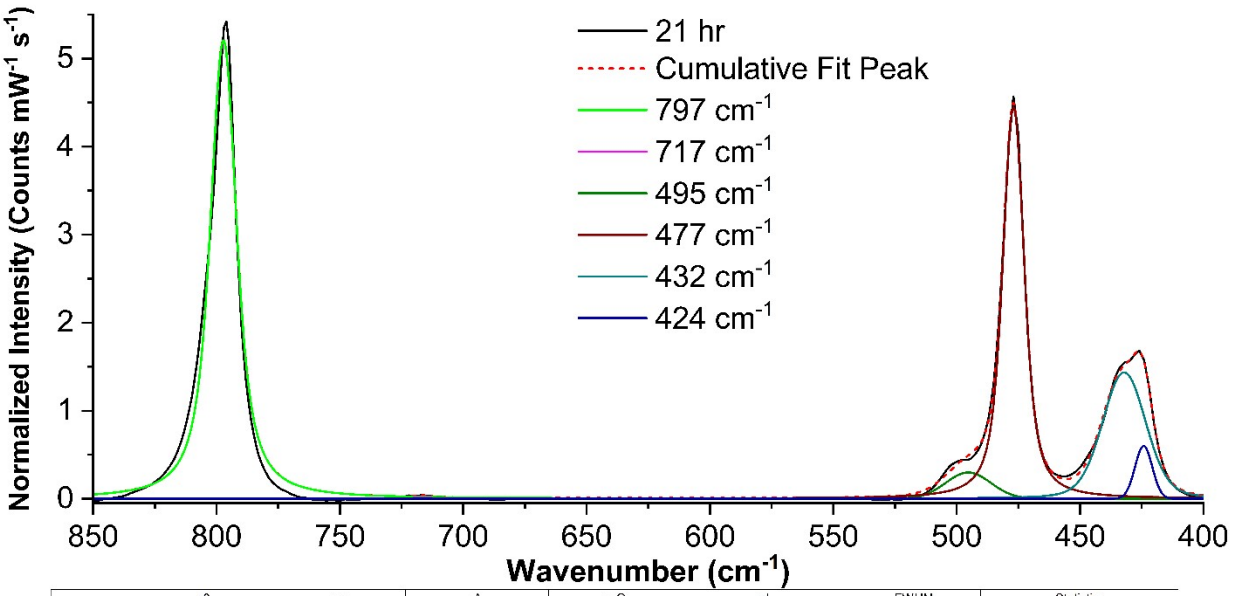

	y0		xc		A		wG		wL		FWHM		Statistics	
	Value	Standard Error	Value	Standard Error	Value	Standard Error	Value	Standard Error	Value	Standard Error	Value	Standard Error	Reduced Chi-Sqr	Adj. R-Square
Peak1(21 hr)	0	0	797.2	0.0463	94.01	0.9622	6.555	0.4437	9.171	0.3433	12.72	0.1647	0.00783	0.9913
Peak2(21 hr)	0	0	716.5	10.57	0.1311	0.6806	7.673	71.92	5.222E-8	101	7.673	28.41		
Peak3(21 hr)	0	0	495.3	1.704	6.838	1.387	21.53	3.902	3.485E-33	1.151E8	21.53	3.902		
Peak4(21 hr)	0	0	477	0.0683	62.04	2.294	6.531	0.5775	6.08	0.6722	10.37	0.1846		
Peak5(21 hr)	0	0	432.1	0.7727	34.73	2.002	18.12	3.122	4.675	3.562	20.75	1.18		
Peak6(21 hr)	0	0	424.2	0.3973	5.254	2.005	8.243	1.466	1E-18	0	8.243	1.466		

Figure S27: Solid-state Raman spectra with fitting parameters and statistics of $[(Co(NH_3)_6)(NpO_4(OH)_2)]\cdot(H_2O)_n$ (n = 2-4) after 21 hours of exposure to acidic vapor.

3. References

(1) Rajapaksha, H.; Benthin, G. C.; Markun, E. L.; Mason, S. E.; Forbes, T. Z. Synthesis, characterization, and density functional theory investigation of $(CH_6N_3)_2[NpO_2Cl_3]$ and $Rb[NpO_2Cl_2(H_2O)]$ chain structures. *Dalton Transactions* **2024**, 10.1039/D3DT03630H. DOI: 10.1039/D3DT03630H.

(2) Augustine, L. J.; Pyrch, M. M. F.; Kravchuk, D. V.; Williams, J. M.; Mason, S. E.; Forbes, T. Z. Density Functional Theory Guided Investigation of Ligand-Induced Neptunyl-Neptunyl Interactions. *European Journal of Inorganic Chemistry* **2023**, *26* (14). DOI: https://doi.org/10.1002/ejic.202200693 (acccessed 2023/05/27).

(3) Kravchuk, D. V.; Augustine, L. J.; Rajapaksha, H.; Benthin, G. C.; Batista, E. R.; Yang, P.; Forbes, T. Z. Insights into the Mechanism of Neptunium Oxidation to the Heptavalent State. *Chemistry* **2024**, *30* (23), e202304049. DOI: 10.1002/chem.202304049 From NLM PubMed-not-MEDLINE.

(4) Bjorklund, J. L.; Pyrch, M. M.; Basile, M. C.; Mason, S. E.; Forbes, T. Z. Actinyl-cation interactions: experimental and theoretical assessment of $[Np(VI)O_2Cl_4]^{2-}$ and $[U(VI)O_2Cl_4]^{2-}$ systems. *Dalton Transactions* **2019**, *48* (24), 8861-8871, 10.1039/C9DT01753D. DOI: 10.1039/C9DT01753D.

(5) Pyrch, M. M.; Bjorklund, J. L.; Williams, J. M.; Parr Iv, D. L.; Mason, S. E.; Leddy, J.; Forbes, T. Z. Impacts of hydrogen bonding interactions with $Np(V/VI)O_2Cl_4$ complexes: vibrational spectroscopy, redox behavior, and computational analysis. *Dalton Transactions* **2020**, *49* (20), 6854-6866, 10.1039/D0DT00848F. DOI: 10.1039/D0DT00848F.

(6) Kovács, A.; Konings, R. J. M.; Gibson, J. K.; Infante, I.; Gagliardi, L. Quantum Chemical Calculations and Experimental Investigations of Molecular Actinide Oxides. *Chemical Reviews* **2015**, *115* (4), 1725-1759. DOI: 10.1021/cr500426s.
(7) de Jong, W. A.; Aprà, E.; Windus, T. L.; Nichols, J. A.; Harrison, R. J.; Gutowski, K. E.; Dixon, D. A. Complexation of the Carbonate, Nitrate, and Acetate Anions with the Uranyl Dication: Density Functional Studies with Relativistic Effective Core Potentials. *The Journal of Physical Chemistry A* **2005**, *109* (50), 11568-11577. DOI: 10.1021/jp0541462.
(8) Li, X.-B.; Wu, Q.-Y.; Wang, C.-Z.; Lan, J.-H.; Ning, S.-Y.; Wei, Y.-Z.; Chai, Z.-F.; Shi, W.-Q. Theoretical Study on the Reduction Mechanism of Np(VI) by Hydrazine Derivatives. *The Journal of Physical Chemistry A* **2020**, *124* (19), 3720-3729. DOI: 10.1021/acs.jpca.0c01504.
(9) Hickam, S.; Ray, D.; Szymanowski, J. E. S.; Li, R.-Y.; Dembowski, M.; Smith, P.; Gagliardi, L.; Burns, P. C. Neptunyl Peroxide Chemistry: Synthesis and Spectroscopic Characterization of a Neptunyl Triperoxide Compound, $Ca_2[NpO_2(O_2)_3]\cdot 9H_2O$. *Inorganic Chemistry* **2019**, *58* (18), 12264-12271. DOI: 10.1021/acs.inorgchem.9b01712.
(10) Yin, Y.-P.; Dong, C.-Z.; Ding, X.-B. Structural and spectral characteristics of neptunyl nitrates $NpO_2(NO_3)_n^q$ (n=1–3, q=+1, 0, −1) and the hydrated complexes $NpO_2(NO_3)_2(H_2O)_m$ (m=1–4). *Chemical Physics Letters* **2015**, *635*, 134-138. DOI: https://doi.org/10.1016/j.cplett.2015.06.048.
(11) Tecmer, P.; Gomes, A. S. P.; Ekström, U.; Visscher, L. Electronic spectroscopy of UO_2^{2+}, NUO^+ and NUN: an evaluation of time-dependent density functional theory for actinides. *Physical Chemistry Chemical Physics* **2011**, *13* (13), 6249-6259, 10.1039/C0CP02534H. DOI: 10.1039/C0CP02534H.
(12) Su, J.; Batista, E. R.; Boland, K. S.; Bone, S. E.; Bradley, J. A.; Cary, S. K.; Clark, D. L.; Conradson, S. D.; Ditter, A. S.; Kaltsoyannis, N.; et al. Energy-Degeneracy-Driven Covalency in Actinide Bonding. *Journal of the American Chemical Society* **2018**, *140* (51), 17977-17984. DOI: 10.1021/jacs.8b09436.
(13) Gendron, F.; Páez-Hernández, D.; Notter, F.-P.; Pritchard, B.; Bolvin, H.; Autschbach, J. Magnetic Properties and Electronic Structure of Neptunyl(VI) Complexes: Wavefunctions, Orbitals, and Crystal-Field Models. *Chemistry – A European Journal* **2014**, *20* (26), 7994-8011. DOI: https://doi.org/10.1002/chem.201305039.
(14) Heaven, M. C.; Barker, B. J.; Antonov, I. O. Spectroscopy and Structure of the Simplest Actinide Bonds. *The Journal of Physical Chemistry A* **2014**, *118* (46), 10867-10881. DOI: 10.1021/jp507283n.
(15) Hu, H.-S.; Wei, F.; Wang, X.; Andrews, L.; Li, J. Actinide–Silicon Multiradical Bonding: Infrared Spectra and Electronic Structures of the $Si(\mu\text{-}X)AnF_3$ (An = Th, U; X = H, F) Molecules. *Journal of the American Chemical Society* **2014**, *136* (4), 1427-1437. DOI: 10.1021/ja409527u.